Bachelor's Thesis in Physics

The Angular Momentum of Kerr Black Holes

Author:
Joakim Bolin
jobo8409@student.su.se

Supervisor:
Prof. Ingemar Bengtsson

Stockholm University

Department of Physics
Stockholm University
Stockholm, Sweden 2015

Abstract

General relativity implies that there is an upper limit on the angular momentum per mass squared of black holes: $J/M^2 \leq 1$, above which the event horizon of a black hole is nonexistent. Thus, it follows from the conservation of angular momentum that hypothetical stars with $J/M^2 > 1$ have to transport at least some of their angular momentum to outer regions in order not to violate the cosmic censorship conjecture. The study of rotational angular momentum for objects such as the Sun thus becomes of great relevance in exploring the stringency of the limit $J/M^2 \leq 1$. Furthermore, when black holes are formed they begin to accrete matter from their surrounding areas, consequently increasing the mass and the angular momentum of the black holes. The limiting value for this process is studied and formulas essential for disk-accretion are explored and derived. The area of the event horizon changes as the mass and the angular momentum of black holes increases, this effect is also studied and analyzed.

Table of Contents

Abstract **2**

Preface **4**

1 Introduction **5**

2 Angular Momentum Distribution in the Solar System **8**
2.1 Rotational & Orbital Angular Momentum 8
2.2 Sidereal Rotation Period & Mass Distribution of the Sun 9
2.3 Distribution of Angular Momentum 10
2.4 The Angular Momentum of other Systems and Particles 11

3 Theoretical Preparations **12**
3.1 Tensor Notation, Minkowski Space & Proper Time 12
3.2 Hamilton's Principle & the Euler-Lagrange Equation 14
3.3 Conservation of Angular Momentum 15
3.4 Rotating Black Holes 15

4 Geodesics in Black Hole Spacetimes **18**
4.1 The Geodesic Equation 18
4.2 The Radial Equation of the Schwarzschild Geometry 20
4.3 Properties of the Kerr Geometry 23

5 Evolution of the Angular Momentum of Black Holes **25**
5.1 Solutions to the Radial Equation of the Kerr Metric 25
5.2 Disk-accretion Onto Black Holes 29
5.3 Accretion for Near Extremal Black Holes 32
5.4 Area of the Event Horizon 33

6 Concluding Remarks **36**

Bibliography **39**

Preface

This thesis has been written with the intention that any third year undergraduate student should be able to understand its topic. Having said so; deriving equations which govern the motion of particles in the vicinity of black holes requires an understanding of general relativity, a subject which few undergraduate students are even remotely familiar with. To circumvent this issue I have created a separate chapter on general relativity with the purpose of deriving the radial equation for Kerr black holes. Therefore, those unfamiliar with general relativity can choose to see for themselves where the radial equation comes from, or simply accept the equation I derive and move on to my analysis of black holes which should be understandable to anyone fluent in the language of analytical mechanics.

Chapter 1 gives an introduction to the main topic of the thesis, chapter 2 deals with the distribution of angular momentum in the solar system. It relies primarily on basic principles found in text books on analytical mechanics, see for an example Goldstein [1], Arnold [2] and my supervisor's *Notes on Analytical Mechanics* [3].

Chapter 3 provides some much needed theoretical preparations and as mentioned earlier; chapter 4 deals with general relativity, and the main purpose of the chapter is to derive the radial equation for Kerr black holes. For this chapter Hartle [4] and Weinberg [5] have been essential in my understanding of the mathematics as well as the physics of general relativity.

In chapter 5 I look for solutions to the radial equation. These are then used for the analysis of the angular momentum of Kerr black holes. It relies primarily on analytical mechanics and therefore does not require the reader to have an understanding of relativity.

Acknowledgements

I would like to thank my supervisor and professor Ingemar Bengtsson for his patience and dedication during the course of this thesis, and for not hesitating to meet me several times a week during periods when I was progressing quickly. I highly recommend him to anyone who is to do their thesis in the future.

An acknowledgement is also due to Dan Kiselman at the Institute of Solar Physics at Stockholm University who provided me with information regarding the rotation of the interior of the Sun.

Chapter 1

Introduction

According to modern physics stars are born from the gravitational attraction within gas clouds which compresses matter into volumes small enough that the pressure becomes so high that thermonuclear fusion ensues. In this manner stars support themselves against the ever present forces of gravity; until such a point that stars run out of thermonuclear fuel. Black holes arise from stars so massive that when they reach the end of their lives gravitational forces become so strong that matter is compressed into volumes small enough that not even light can escape them.

Supermassive black holes found in the center of galaxies do not arise from the gravitational collapse of individual stars, their formation is an open field of research. Some theories involve the gravitational collapse of millions of stars, the interaction and fusion of smaller black holes and perhaps even dark matter.

Black holes can rotate, and such black holes consequently carry an angular momentum J. A dimensionless quantity of great interest is cJ/GM^2, where c is the speed of light, G is the gravitational constant and M is the mass of the rotating object. It is customary to use geometrized units $c = G = 1$, which effectively redefines angular momentum to be measured in units of length squared, and mass to be measured in units of length. Geometrized units will from here on be assumed, and our focus will be on the dimensionless quantity J/M^2.

The Kerr metric describes rotating black holes which carry an angular momentum per mass a, where $a \equiv J/M$ is the Kerr parameter and we define $\tilde{a} \equiv a/M$. The angular momentum per mass squared varies between $-1 \leq \tilde{a} \leq 1$, where the negative sign is for particles in counterrotation with black holes. The limitation on $\tilde{a}$ of black holes arises as a consequence of the general theory of relativity. Static black holes on the other hand which do not carry angular momentum, $J = 0$, can be adequately described by the Schwarzschild metric. The study of general relativity and relevant spacetime geometries for black holes is the topic of chapter 4.

The limitation $\tilde{a} \leq 1$ does not exist for other objects such as the Sun or the elementary particles. In principle then, we may find massive stars which carry an angular momentum per mass squared $\tilde{a} > 1$. Thus, an interesting phenomenon to study is what would happen to such a hypothetical star as it becomes singular at the end of its life; from the conservation of angular momentum it follows that if a star with $\tilde{a} > 1$ collapses and become singular, there has to exist some process which transports angular momentum outwards in order not to violate the limit $\tilde{a} \leq 1$ for the black hole. The study of such processes is not the topic of this thesis, and we shall only briefly discuss how the angular momentum could be transported in a direction outwards from the black hole in order not to violate this limit.

Because black holes have a limitation on their angular momentum per mass squared, it becomes of great importance to analyze $\tilde{a}$ of rotating objects such as stars. This is the topic of chapter 2, and we shall see that calculations seem to imply that the Sun has an angular

momentum per mass squared $\tilde{a} \approx 0.23$. There are several examples in which $\tilde{a} \gg 1$, such an example is the electron which has a value $\tilde{a} \sim 10^{44}$, it is thus clear that an angular momentum per mass squared $0 \leq \tilde{a} \leq 1$ is not in any way a constraint which applies to all rotating objects, hence there is no obvious reason to assume that there doesn't exist stars with $\tilde{a} > 1$.

The solar system has a value of $\tilde{a} \gg 1$ more precisely the total angular momentum per mass squared of the solar system has a value around $\tilde{a} \approx 36$, as will be seen in chapter 2. Thus if the solar system arose out of a massive gas cloud it seems clear that processes which transport angular momentum outwards in the system operated on it in its early days.

The event horizon of a black hole is defined as the null three-surface inside which no particle can escape the black hole, and outside this surface particles can carry information to distant observers. The singularity of a black hole lies inside the event horizon and can therefore not be observed. No rigorous proof from Einstein's equations has been formulated to show that a singularity is always hidden inside the event horizon. In 1969 Roger Penrose argued that this always happens, a conjecture known as the **cosmic censorship hypothesis**.

The event horizon and the angular momentum per mass squared of black holes are closely related. The radius of the event horizon is in fact a function of $\tilde{a}$, and in chapter 4 we will show that the radius of the event horizon for $0 \leq \tilde{a} \leq 1$ varies according to $M \leq r \leq 2M$, decreasing as $\tilde{a}$ increases. In principle the Kerr geometry of general relativity allows for $\tilde{a} > 1$, but in this case there is no real solution for the radius of the event horizon. In other words, for a hypothetical black hole with $\tilde{a} \geq 1$, cosmic censorship is violated and there is no longer an event horizon.

Some distance outside the event horizon of black holes there exist stable solutions to the orbit of particles. The innermost of these is known as the innermost stable circular orbit denoted r_{ISCO}. From this radius and outwards there exist particles which make up a disk of gas in orbit around black holes, these particles carry both energy and angular momentum. Suppose that from this disk, particles are being dumped directly down into a black hole. In this manner the black hole accretes matter which causes the mass of the black hole and the angular momentum per mass squared of the black hole to increase (see Bardeen, [12] and Thorne, [17]). In principle then we could imagine that a black hole with some initial value of $\tilde{a}_0$, with sufficient amounts of matter in the vicinity of the black hole, could accrete matter until cosmic censorship is violated, and acquire a value $\tilde{a} > 1$. This special example of disk-accretion is the topic of chapter 5, and it will there be argued that the angular momentum per mass squared can never reach values $\tilde{a} > 1$ from this process of disk-accretion; rendering cosmic censorship inviolable.

There are several other processes which can change the angular momentum of black holes. These will be mentioned briefly in chapter 5, however we shall not make an in-depth study of these in this thesis.

In chapter 4 it will be shown that r_{ISCO} is also a function of the angular momentum much like the radius of the event horizon. More precisely for $0 \leq \tilde{a} \leq 1$, r_{ISCO} varies according to $M \leq r_{\text{ISCO}} \leq 6M$, decreasing as $\tilde{a}$ increases. However, astrophysical complications such as radiation arising in the process of accretion causes the limit $\tilde{a} = 1$ to never be reached (see Thorne, [17] which gives an upper limit $\tilde{a} = 0.998$). Observations imply that $\tilde{a} \approx 0.9$ for supermassive black holes and in some cases perhaps even higher [7, 8].

In section 5.2 we will derive an equation (originally derived by Bardeen [12]) which gives the evolution of $\tilde{a}$ as a function of M, and it turns out that the greater $\tilde{a}$ becomes the faster M increases. More precisely the equation tells us that near extremal black holes require more mass to increase their angular momentum per mass squared by the same amount as say, near static black holes.

The event horizon has several interesting properties. One of those is how the area of the event horizon varies as a function of angular momentum per mass squared. It turns out that the area of the event horizon is a function of both the angular momentum per mass squared $\tilde{a}$ and the mass ratio of the black hole M/M_1 where M_1 is the mass of the black hole before it has accreted any mass, M is then the total mass at any given time later. In principle it turns out that increasing $\tilde{a}$ actually decreases the area of the event horizon when the mass ratio M/M_1 is held fixed. However as we discussed in the previous paragraph an increase in $\tilde{a}$, from the process of disk-accretion we study, is *always* coupled with an increase in the mass ratio M/M_1. Since the increase in mass of black holes becomes larger the higher the angular momentum per mass squared becomes, the net effect is regardless an increase in the area of the event horizon, despite the fact that contributions from the angular momentum *itself*, actually decreases the area.

Chapter 2

Angular Momentum Distribution in the Solar System

This chapter is devoted to the study of the angular momentum of the Sun and its distribution in the solar system. A first approximation is made to the rotational angular momentum of the Sun, where we assume that the Sun is a homogeneous sphere with constant angular frequency, or sidereal rotation period. We then compare this result with a more accurate calculation which accounts for variations in the mass distribution as well as the sidereal rotation period of the Sun. We move on to investigate how the angular momentum of the solar system is distributed with the radius from the Sun, and finally we explore the angular momentum of some other systems and particles.

2.1 Rotational & Orbital Angular Momentum

The **rotational angular momentum** J_{rot} with respect to the origin of a homogeneous sphere spinning around its own axis is given by:

$$J_{\text{rot}} = \frac{4\pi M R^2}{5T}, \tag{2.1}$$

where M is the mass of the rotating object, R is its radius and T its sidereal rotation period.

We seek to investigate the distribution of the angular momentum in the entire system so we will also be interested in the **orbital angular momentum** J_{orb} given by the equation:

$$J_{\text{orb}} = \frac{2\pi m R^2}{T}. \tag{2.2}$$

Kepler's third law relates the semi-major axis a of an object to its orbital period T according to

$$T = 2\pi \left(\frac{a^3}{GM} \right)^{1/2}, \tag{2.3}$$

where G is the gravitational constant and M is the mass of the star which the object orbits. For circular motion we have simply that $a = R$, and with this in mind we modify Eq. (2.2):

$$J_{\text{orb}} = m(GMR)^{1/2}, \tag{2.4}$$

where m is the mass of the planet in orbit around the star.

2.2 Sidereal Rotation Period & Mass Distribution of the Sun

It turns out that the assumption made in the previous section related to approximating the density of the Sun as a homogeneous sphere lead to inaccurate results in estimating the structure of stellar objects and consequently in the estimation of the angular momentum of the Sun.

In order to estimate the rotational angular momentum of the Sun we require an understanding of how its density varies with the radius as well as how the angular frequency, or sidereal rotation period, varies with both latitude and radius. The latter of these have been studied by Howe [13], and it turns out that the sidereal rotation period has a rather peculiar behavior; seemingly almost constant at a radius $r/R_{\text{Sun}} < 0.5$ and varying greatly in the outer regions with both radius and latitude. The former has been studied by Christensen-Dalsgaard et al. [14], and it has been shown that the density distribution decreases rapidly with the radius of the Sun as seen in Fig. 2.1.

Consequently then, it turns out that calculation of the rotational angular momentum of the Sun is a tricky business. No obvious conclusion can be drawn either in regards to whether the angular momentum of the Sun will be lower or higher compared to an approximation in which we assume that the Sun is a homogeneous sphere with constant angular frequency. Consider for an example the argument that the angular momentum ought to be much lower than a homogeneous sphere approximation as a consequence of the rapid decrease in the Suns density. Such an argument would hold if the angular frequency was shown to remain constant or decrease rapidly at the outer layers. However no such results exist; as we previously discussed the angular frequency of the Sun seem to increase at the outer layers, hence no obvious conclusion can be made in regards to the contribution to the angular momentum in the outer layers of the Sun.

Since the purpose of this thesis isn't to provide an accurate calculation of the angular momentum of the Sun; we will not dig deeper into the mathematics of stellar structure here, but instead refer to a calculation made by Pia Di Mauro [15]*. The calculation shows that the rotational angular momentum of the Sun has a value in the vicinity of $J_{\text{rot}} = 2.0 \cdot 10^{41}\,\text{kgm}^2\text{s}^{-1}$ which surprisingly, and perhaps also coincidentally,

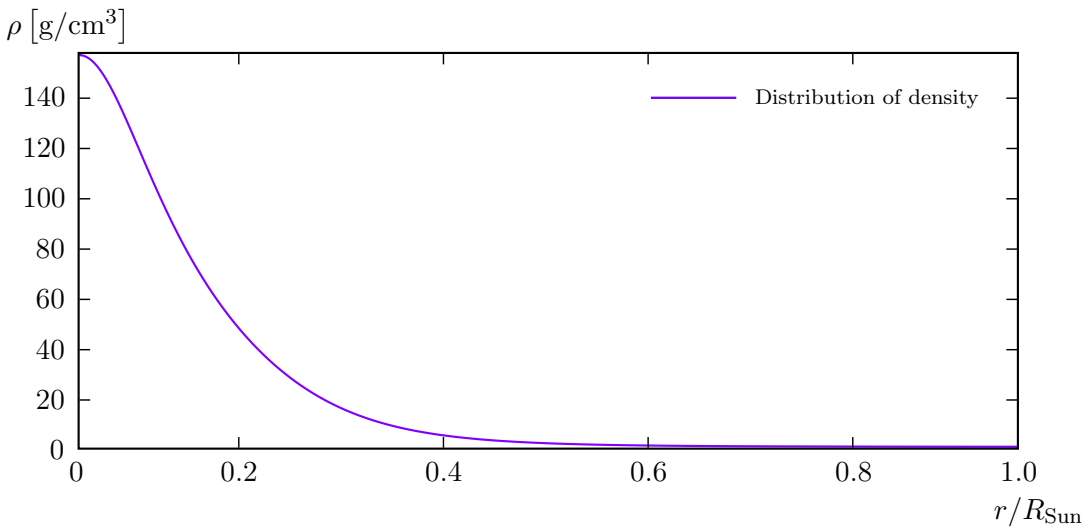

Figure 2.1: Distribution of the density ρ of the Sun as a function of its radius r, based on data from the Global Oscillation Network Group (GONG). The density decreases rapidly with the radius of the Sun, and as a consequence of the definition of angular momentum the contribution from outer layers is lower compared to what we would get from a homogeneous sphere approximation.

*Pia Di Mauro also provides a figure for the angular frequency variation within the Sun.

is rather close to the actual angular momentum we get from a homogeneous sphere approximation with constant sidereal rotation period. Using Eq. (2.1), gives us a value for $J_{\text{rot}} = 1.1 \cdot 10^{42}\,\text{kgm}^2\text{s}^{-1}$, hence a homogeneous sphere approximation seem to give us a slight overestimation.

2.3 Distribution of Angular Momentum

From the discussion in the previous section we find that the Sun has a value $J/M_\odot^2 \approx 1.3$ for a homogeneous sphere approximation and $J/M_\odot^2 \approx 0.23$ for the calculation made by Pia Di Mauro. In other words the angular momentum per mass squared of the Sun appears to lie well within the limit $\tilde{a} \leq 1$.

In order to study the distribution of the angular momentum of the solar system we now move on to calculate the orbital angular momentum of the planets. Using Eq. (2.2) we can calculate the values for all the planets in the solar system*, and add these values up as we move further out. In this manner, we can plot the discrete values of the distribution of the angular momentum as a function of the radius from the Sun which is demonstrated in Fig. 2.2. From this figure it is clear that the majority of the angular momentum comes from Jupiter, while the inner planets make almost no contribution, and the outer planets Saturn, Neptune and Uranus adds to it slightly. All this, regardless of the fact that the Sun is about a thousand times more massive.

From Fig. 2.2 arises an interesting question regarding how the solar system came to have its angular momentum distributed so far from its center. From conservation laws follows that the total angular momentum of the gas cloud which the solar system originates from has to be the same as it is today. Given that the solar system arose out of a massive gas cloud; there is a sign here of some process which has transported the majority of the angular momentum to the outer regions.

The reader may ask why we have neglected contributions from the Kuiper belt objects in Fig. 2.2. The reason is quite simple; despite its vast extent the total mass of the Kuiper belt is much lower than the mass of the earth. A calculation then shows that the Kuiper

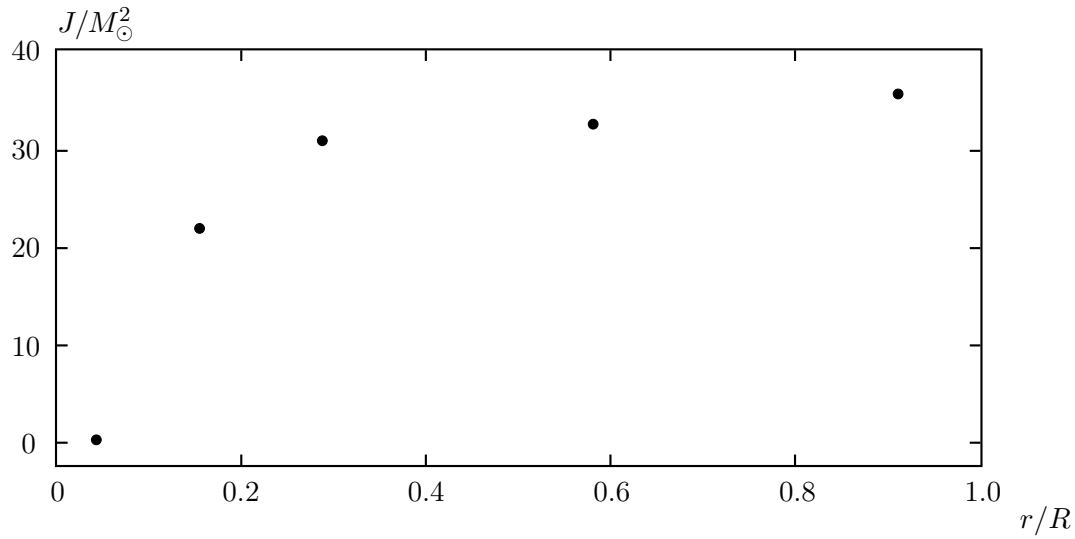

Figure 2.2: The figure displays the distribution of the quantity $J/M_\odot^2$ as a function of the radius r/R where $R \equiv 5 \cdot 10^{12}$ m. The dots represent the distribution of the angular momentum per mass squared near various objects in the solar system in the order of: Mars, Jupiter, Saturn, Uranus and Neptune. The angular momentum per mass squared for planets prior to Mars is included in the value for Mars, but as can be seen all contributions prior to Jupiter are insignificant.

*For astronomical data, see for an example Physics Handbook.

belt has no significant impact on the angular momentum of the solar system and has therefore been neglected here.

It would be valuable to examine other solar systems with the purpose of investigating whether the same pattern repeats itself or not, that is to say if other systems also has the majority of their angular momentum in the outer regions. Other systems are of course known but unfortunately they are not known to the same accuracy as our own system.

2.4 The Angular Momentum of other Systems and Particles

It is clear that the angular momentum of the Sun-Jupiter system has the vast majority of its angular momentum at Jupiter. Moving on, we can in a similar manner look at the Earth-Moon system. By calculating the rotational angular momentum of the Earth and comparing it to the orbital angular momentum of the Moon, we find a value $J_{\text{rot}} = 7 \cdot 10^{33}\,\text{kgm}^2\text{s}^{-1}$ for the Earth and a value $J_{\text{orb}} = 3 \cdot 10^{34}\,\text{kgm}^2\text{s}^{-1}$ for the Moon. Hence we find the same pattern for the Earth-Moon system as we did for the Sun-Jupiter system; the angular momentum appears to be distributed far away from the central body.

Just as we calculated $J/M_{\odot}^2$ for the Sun we can do the same for the Earth and Jupiter. For the Earth we find a value $J/M_{\oplus}^2 \approx 890$ and for Jupiter we find $J/M^2 \approx 850$. Jupiter is of course not a rigid body so the value of J/M^2 given here may not be accurate. The value for the Earth on the other hand should not deviate much from the actual value, since a rigid body approximation applies fairly well to the Earth. Furthermore we can do the same calculation for the elementary particles such as the electron which has a z–component of its angular momentum $J_z = \frac{1}{2}\hbar$, and we then find that $J_z/M^2 \approx 1.5 \cdot 10^{44}$.

From these calculations it is clear that there exist plenty of objects in the universe which have an angular momentum per mass squared $\tilde{a} > 1$, and it isn't especially difficult to think of other examples. Hence there is no obvious reason to assume that all or even most stars have an angular momentum per mass squared $\tilde{a} \leq 1$.

Chapter 3

Theoretical Preparations

In this chapter we lay the groundworks to furnish calculations which are to come. General relativity relies heavily on tensor notation and it is therefore appropriate to begin by giving a brief summary of the Einstein summation convention, and followed by this is a definition of the proper time. From Hamilton's principle it is possible to derive the Euler-Lagrange equation which gives the equations of motion for particles in spacetime, and from the Lagrangian formalism follows the definition of canonical momentum from which it is easy to show that angular momentum is conserved for central forces. Finally we summarize some historical aspects of rotating black holes as well as some of the most important formulas used and derived in this thesis for rotating black holes.

Greek letters $\mu, \nu, \kappa, \lambda$ will always be taken as indices running over the four spacetime coordinates, in example (t, x, y, z) or (t, r, θ, ϕ). Latin letters i, j, k are used as indices for the three spatial dimensions and usually run over coordinates (x, y, z) or (r, θ, ψ).

3.1 Tensor Notation, Minkowski Space & Proper Time

In this thesis we will make use of the Einstein summation convention where it is due. When two indices are repeated in the same term summation will be understood and we will neglect the summation sign.

As an example consider a Minkowski space with the sign convention $(-, +, +, +)$, which has the **covariant metric**:

$$g_{\mu\nu} = \begin{pmatrix} -1 & 0 & 0 & 0 \\ 0 & 1 & 0 & 0 \\ 0 & 0 & 1 & 0 \\ 0 & 0 & 0 & 1 \end{pmatrix}, \tag{3.1}$$

where the metric $g_{\mu\nu}$ is a tensor. Let $x^\mu = (ct, x, y, z)^\intercal$ be our coordinates, the lineelement for flat spacetime is then given by the scalar product:

$$ds^2 = dx_\mu dx^\mu = g_{\mu\nu} dx^\mu dx^\nu = -(cdt)^2 + dx^2 + dy^2 + dz^2, \tag{3.2}$$

Here, written in downstairs notation, dx_μ is called a **covariant vector*** meanwhile dx^μ, written in upstairs notation, is called a **contravariant vector**. The metric thus allows us to express a covariant vector as $x_\mu = g_{\mu\nu} x^\nu$ and similarly there exists a **contravariant inverse** $g^{\mu\nu}$ which gives a contravariant vector according to $x^\mu = g^{\mu\nu} x_\nu$.

Another important property to mention is that multiplying a covariant metric with its contravariant inverse produces the following result:

$$g^{\mu\kappa} g_{\kappa\nu} = \delta^\mu{}_\nu, \tag{3.3}$$

*A covariant vector is also called a **1-form**, in this language the contravariant vector is called just a vector.

where $\delta^{\mu}_{\ \nu}$ defines an operation which acts as the identity on both a covariant vector: $x_\nu = x_\mu \delta^{\mu}_{\ \nu}$ and a contravariant vector: $x^\nu = \delta^{\nu}_{\ \mu} x^\mu$.

Frequently we will make use of the following short hand notation for partial derivatives:

$$\partial_\mu \equiv \frac{\partial}{\partial x^\mu}, \tag{3.4}$$

and similarly there exists a contravariant analogue given by:

$$\partial^\mu \equiv \frac{\partial}{\partial x_\mu}, \tag{3.5}$$

however we will not make use of the latter in this thesis. Regardless, there should be no confusion when such expressions arise.*

Let us now make a change of coordinates in Eq. (3.2) to spherical coordinates, then $(ct, x, y, z) \to (ct, r, \theta, \phi)$ and the same lineelement takes the form:

$$ds^2 = -(cdt)^2 + dr^2 + r^2 \left(d\theta^2 + \sin^2\theta \, d\phi^2\right), \tag{3.6}$$

and consequently the metric in Eq. (3.1) must also change, written out explicitly it becomes:

$$g_{\mu\nu} = \begin{pmatrix} -1 & 0 & 0 & 0 \\ 0 & 1 & 0 & 0 \\ 0 & 0 & r^2 & 0 \\ 0 & 0 & 0 & r^2 \sin^2\theta \end{pmatrix}. \tag{3.7}$$

Let us again examine the lineelement for the Minkowski space in Eq. (3.2). The sign-convention employed in Eq. (3.1) portrays the fact that the spacetimes of general relativity are *not* four-dimensional Euclidean geometries. This has far reaching consequences and we have in particular for two different points that they can be separated by distances ds^2 that take values which are positive, negative or zero. For values of $ds^2 > 0$ we say that the points are **spacelike separated**, for $ds^2 = 0$ we say that they are **null separated** and in the case when $ds^2 < 0$ we say that they are **timelike separated**.

Particles which travel on timelike world lines are timelike separated, and we define such world lines by the differential:

$$d\tau^2 \equiv -\frac{ds^2}{c^2}, \tag{3.8}$$

the differential $d\tau$ is then measured in units of time and we refer to τ as the **proper time**, which is the time that a clock would measure along the world line. In this thesis we will only concern ourselves with timelike world lines, with a minor exception for the event horizon of black holes which is made up of lightlike (null) world lines.†

It is convenient, for reasons which shall become clear later on, to use **geometrized units** where the gravitational constant G and the speed of light c is set so that $c = G = 1$, this effectively redefines mass to be measured in units of length. A dimensionless quantity of great interest is $\tilde{a} = a/M = J/M^2$, where a is called the **Kerr parameter** (see chapter 4 for more information regarding this parameter).

Using geometrized units, or perhaps rather $c = 1$ units, we now see from Eq. (3.8) that $ds^2 = -d\tau^2$. If we plug this into Eq. (3.2) for the lineelement of the Minkowski space it turns into:

$$d\tau^2 = dt^2 - dx^2 - dy^2 - dz^2, \tag{3.9}$$

we could now apply Hamilton's principle to the corresponding Lagrangian and arrive at the equations of motion for timelike geodesics for a relativistic free particle. The general equations of motion for an arbitrary spacetime is derived in chapter 4, and we now move on to describe the necessary tools for this procedure.

*For a more detailed discussion see Bengtsson [3], p. 88 and [6] on special relativity.

†See also chapter 4 in Hartle [4] for a discussion on light cones etc.

3.2 Hamilton's Principle & the Euler-Lagrange Equation

One of the arguably most beautiful facts in all of physics is that particles travel along paths in which the corresponding action functional has an extremal value, more precisely, the equations of motion for particles can be derived by minimizing the action functional. We let this action functional, which is a function of a function, be given as:

$$\mathcal{S}[x^\mu(\sigma)] = \int_{\sigma_1}^{\sigma_2} d\sigma\, L\left(\frac{dx^\mu}{d\sigma}, x^\mu\right), \tag{3.10}$$

where the $x^\mu(\sigma)$'s are arbitrary paths which the particles can take in spacetime and $L\left(dx^\mu/d\sigma, x^\mu\right)$ is the **Lagrangian**.

We now claim that the specific path which the particles take can be derived from the condition $\delta\mathcal{S} = 0$ so that

$$\delta\mathcal{S} = \delta\int_{\sigma_1}^{\sigma_2} d\sigma\, L\left(\frac{dx^\mu}{d\sigma}, x^\mu\right) = 0. \tag{3.11}$$

This is known as **Hamilton's Principle** and by evaluation of this expression it is possible to derive the **Euler-Lagrange equation** which yields the equations of motion:

$$\frac{\partial L}{\partial x^\mu} - \frac{d}{d\sigma}\left(\frac{\partial L}{\partial\left(dx^\mu/d\sigma\right)}\right) = 0. \tag{3.12}$$

To prove this we restrict ourselves to functions, and indeed these are the only functions which will be of interest to us, in which there exist values $x^\mu(\sigma_1)$ and $x^\mu(\sigma_2)$ which are held fixed under variation of the functions $x^\mu(\sigma)$. We now turn to the calculus of variation and notice that a necessary condition for an extremum is that

$$\delta L = \delta x^\mu \frac{\partial L}{\partial x^\mu} + \delta\left(\frac{dx^\mu}{d\sigma}\right)\frac{\partial L}{\partial\left(dx^\mu/d\sigma\right)} = 0. \tag{3.13}$$

Consequently we then find that a variation of the action in Eq. (3.10) results in:

$$\delta\mathcal{S} = \int_{\sigma_1}^{\sigma_2} d\sigma\left[\delta x^\mu \frac{\partial L}{\partial x^\mu} + \delta\left(\frac{dx^\mu}{d\sigma}\right)\frac{\partial L}{\partial\left(dx^\mu/d\sigma\right)}\right] = 0, \tag{3.14}$$

and we now wish to transform the integrand in such a way that it is expressed in terms of δx^μ and to this end we perform a partial integration in the second term and find instead:

$$\delta\mathcal{S} = \int_{\sigma_1}^{\sigma_2} d\sigma\delta x^\mu\left[\frac{\partial L}{\partial x^\mu} - \frac{d}{d\sigma}\left(\frac{\partial L}{\partial\left(dx^\mu/d\sigma\right)}\right)\right] + \left[\delta x^\mu \frac{\partial L}{\partial\left(dx^\mu/d\sigma\right)}\right]_{\sigma_1}^{\sigma_2} = 0. \tag{3.15}$$

From the conditions made earlier it is clear that the boundary term must vanish since the end points are held fixed; so the variation here must be zero. Furthermore we require that the variation of the action is zero regardless of how we choose δx^μ, and if this is to be true then the integrand must always be zero, so we have in fact shown that

$$\frac{\partial L}{\partial x^\mu} - \frac{d}{d\sigma}\left(\frac{\partial L}{\partial\left(dx^\mu/d\sigma\right)}\right) = 0, \tag{3.16}$$

which is exactly the Euler-Lagrange equation given in Eq. (3.12). Q.E.D.

3.3 Conservation of Angular Momentum

Let us direct our attention to central force motion. Suppose we have been given some Lagrangian $L = T - V$, where T is the kinetic energy and V is the potential energy. Since we are dealing with a central force the potential is a function of the radius only. Consequently then:

$$\frac{\partial L}{\partial \dot{x}_i} = \frac{\partial T}{\partial \dot{x}_i} = m\dot{x}_i \equiv p_i. \tag{3.17}$$

Here p_i is defined as the **canonical momentum** and we have:

$$p_i \equiv \frac{\partial L}{\partial \dot{x}_i}. \tag{3.18}$$

Based on this we now wish to show that there exists a conserved quantity:

$$J_i = m\epsilon_{ijk} x_j \dot{x}_k, \tag{3.19}$$

where ϵ_{ijk} is the Levi-Cevita symbol and J_i is the angular momentum. Taking advantage of spherical symmetry we now choose spherical coordinates (r, θ, ψ), where θ is the azimuth angle and ψ is the polar angle. We now choose the polar axis in such a way that it is always in the direction of J_i, the polar angle ψ is then always $\pi/2$ and can hence be dropped from the discussion. The Lagrangian now becomes:

$$L(r, \dot{r}, \dot{\theta}) = \frac{1}{2} m \left(\dot{r}^2 + r^2 \dot{\theta}^2 \right) - V(r), \tag{3.20}$$

hence θ is a cyclic coordinate and using Eq. (3.18) we find:*

$$\frac{\partial L}{\partial \dot{\theta}} = m r^2 \dot{\theta} = l, \tag{3.21}$$

where l is the constant magnitude of the angular momentum, which is easy to verify since:

$$\frac{d}{dt}\left(\frac{\partial L}{\partial \dot{\theta}} \right) = \frac{d}{dt}\left(m r^2 \dot{\theta} \right) = 0, \tag{3.22}$$

and it is thus clear that for central forces there exists a conserved quantity in accordance with Eq. (3.19). Q.E.D.

3.4 Rotating Black Holes

Shortly after Albert Einstein published the general theory of relativity in 1916, Karl Schwarzschild used the Einstein vacuum equation to derive a metric which describes a static black hole. The metric is called the **Schwarzschild metric** and is given by the lineelement:

$$ds^2 = -\left(1 - \frac{2M}{r}\right) dt^2 + \left(1 - \frac{2M}{r}\right)^{-1} dr^2 + r^2 \left(d\theta^2 + \sin^2\theta \, d\phi^2 \right). \tag{3.23}$$

This metric describes a black hole with a center at $r = 0$ since as the radius approaches zero, the curvature of spacetime approaches a singularity. This can be seen easily in the first part of the lineelement in Eq. (3.23) since for $r \to 0$ we have that $(1 - 2M/r) \to -\infty$.

There is another singularity in the lineelement at $r = 2M$, however this singularity turns out to be a consequence of the choice of coordinates and there is no actual singularity

*See also Noether's theorem; Goldstein [1], p. 589.

in spacetime. There is however something else of great interest happening at this point. The radius $r = 2M$ defines the null three-surface of a black hole inside which no particle can escape it, and outside this region a particle can carry information to an observer at infinity. The three-surface defined by the radius $r = 2M$ is called the **event horizon** of Schwarzschild black holes.

By using various symmetry properties, it is possible to derive a radial equation for equatorial motion given by:

$$\frac{e^2 - 1}{2} = \left(\frac{dr}{d\tau}\right)^2 + V_{\text{eff}}(r), \tag{3.24}$$

where the effective potential $V_{\text{eff}}(r)$ is given by:

$$V_{\text{eff}}(r) = \frac{\ell^2}{2r^2} - \frac{M}{r} - \frac{M\ell^2}{r^3}. \tag{3.25}$$

Here e is the **energy per unit rest mass** and ℓ is the **angular momentum per unit rest mass** for a particle in the vicinity of the black hole. For more information regarding the Schwarzschild metric see chapter 4.

Many years later in 1963, Roy Kerr published a paper [9] in which he provided solutions to the Einstein equation; a metric which describes a rotating collapsed object with angular momentum per mass a. Later on in 1969, Donald Lynden-Bell published a paper [11] which suggested that black holes could be located at the center of galaxies, with a geometry described by the Schwarzschild metric. In 1970 James M. Bardeen responded by publishing a landmark paper [12] which suggested that the Schwarzschild metric would likely be inadequate in such a description since it does not allow for angular momentum. Bardeen argued that a black hole would be described by the metric derived by Kerr, called the **Kerr metric** and in Boyer-Lindquist coordinates (t, r, θ, ϕ) [10], given by the lineelement:

$$\begin{aligned} ds^2 = &-\left(1 - \frac{2Mr}{\rho^2}\right) dt^2 - \frac{4Mar\sin^2\theta}{\rho^2} d\phi dt + \frac{\rho^2}{\Delta} dr^2 + \rho^2 d\theta^2 \\ &+ \left(r^2 + a^2 + \frac{2Mra^2\sin^2\theta}{\rho^2}\right)\sin^2\theta\, d\phi^2, \end{aligned} \tag{3.26}$$

where, as mentioned earlier, the parameter $a \equiv J/M$ is called the Kerr parameter, $\rho^2 \equiv r^2 + a^2\cos^2\theta$ and $\Delta = r^2 - 2Mr + a^2$.

The Kerr metric is not spherically symmetric, only axisymmetric. The general orbit in the Kerr geometry will therefore not lie in a plane. However, there still exist orbits in the equatorial plane and we will restrict our attention to such orbits for which $\theta = \pi/2$. It is then possible to generalize the effective potential in Eq. (3.25) for the Schwarzschild metric:

$$V_{\text{eff}}(r) = \frac{\ell^2 - a^2(e^2 - 1)}{2r^2} - \frac{M\left(\ell - ae\right)^2}{r^3} - \frac{M}{r}. \tag{3.27}$$

For more information regarding the Kerr metric see chapter 4.

Bardeen went on to find solutions for e, ℓ and $\tilde{a} \equiv a/M$ resulting in three simple expressions valid for the **radius of the innermost stable circular orbit** r_{ISCO}:

$$e(z) = \left(1 - \frac{2}{3z}\right)^{1/2}, \tag{3.28a}$$

$$\ell(z, M) = \frac{2M}{3^{3/2}}\left[1 + 2(3z - 2)^{1/2}\right], \tag{3.28b}$$

$$\tilde{a}(z) = \frac{1}{3}z^{1/2}\left[4 - (3z - 2)^{1/2}\right]. \tag{3.28c}$$

where $z \equiv r_{\mathrm{ISCO}}/M$, equations which he ultimately used to find a relation between z and the mass M of black holes:

$$\frac{z}{z_1} = \left(\frac{M_1}{M}\right)^2, \tag{3.29}$$

where z_1 and M_1 are the initial values at $\tilde{a} = 0$. By using Eq. (3.29) in Eq. (3.28c) Bardeen then derived an expression for how the angular momentum per mass squared of black holes changes with their mass:

$$\tilde{a}(M) = \left(\frac{2}{3}\right)^{1/2} \frac{M_1}{M} \left\{ 4 - \left[18 \left(\frac{M_1}{M}\right)^2 - 2 \right]^{1/2} \right\}. \tag{3.30}$$

Black holes are generally surrounded by an accretion disk and the inner edge of this disk is located at r_{ISCO}. Eq. (3.30) is valid under the condition that particles are being dumped directly down into black holes from the accretion disk at r_{ISCO}, with energy per unit rest mass and angular momentum per unit rest mass satisfied by Eq. (3.28a) and Eq. (3.28b). In this manner the mass and the angular momentum per mass squared increases as particles are accreted onto black holes.

The papers Bardeen published in 1970 [12] and later in 1972 [16], gave only sketchy derivations. Kip Thorne later added some information in 1974 [17], but his derivations were sketchy as well. This thesis gives the full details on the derivations, and these can be found in chapter 5.

Chapter 4

Geodesics in Black Hole Spacetimes

We start this chapter by deriving the geodesic equation from an arbitrary spacetime, with an arbitrary metric $g_{\mu\nu}$ from Hamilton's principle. In Einstein's theory of general relativity the world lines for particles "in free fall" are always geodesics.

We then move on to examine the Schwarzschild metric which describes a static black hole and the Kerr metric which describes a rotating black hole with angular momentum per mass a. From these metrics it is possible to find constants of the motion in the form of energy per unit rest mass and angular momentum per unit rest mass. These constants can then be used to find solutions to the geodesic equation; radial equations which govern the motion of particles in the vicinity of black holes.

This chapter is provided for completeness. If you are familiar with general relativity you can move on to chapter 5.

4.1 The Geodesic Equation

Using the Euler-Lagrange equation we now wish to derive the **geodesic equation**. Let us examine some arbitrary timelike metric:

$$d\tau^2 = -g_{\mu\nu} dx^\mu dx^\nu, \tag{4.1}$$

with the corresponding action:

$$\mathcal{S}'[x^\mu(\sigma)] = \int_{\sigma_1}^{\sigma_2} d\sigma \left(-g_{\mu\nu} \frac{dx^\mu}{d\sigma} \frac{dx^\nu}{d\sigma} \right)^{1/2}, \tag{4.2}$$

where we let the mass of the particle $m = 1$,* and we assume that the end points σ_1 and σ_2 are held fixed under variation. The Lagrangian for this action is:

$$L'\left(\frac{dx^\mu}{d\sigma}, x^\mu \right) = \left(-g_{\mu\nu} \frac{dx^\mu}{d\sigma} \frac{dx^\nu}{d\sigma} \right)^{1/2}, \tag{4.3}$$

and from it we seek the equations of motion. But, observantly we notice that variation of the action in Eq. (4.2) yields the same equations of motion as variation of the following action:

$$\mathcal{S}[x^\mu(\sigma)] = \int_{\sigma_1}^{\sigma_2} d\sigma \left(\frac{1}{2} g_{\mu\nu} \frac{dx^\mu}{d\sigma} \frac{dx^\nu}{d\sigma} \right), \tag{4.4}$$

where the corresponding Lagrangian is:

$$L\left(\frac{dx^\mu}{d\sigma}, x^\mu \right) = \frac{1}{2} g_{\mu\nu} \frac{dx^\mu}{d\sigma} \frac{dx^\nu}{d\sigma}. \tag{4.5}$$

*Note that this won't cause us any trouble because when the corresponding Lagrangian is applied to the Euler-Lagrange equation we can divide by m anyway.

The proof amounts to showing that extremizing the action functionals in Eq. (4.2) and Eq. (4.4) produces the same equations of motion. We assume that the metric is invertible, that is to say, that there exist a contravariant inverse $g^{\mu\kappa}$ such that

$$g^{\mu\kappa} g_{\kappa\nu} = \delta^{\mu}{}_{\nu}, \tag{4.6}$$

Furthermore we assume that the metric is symmetric; $g_{\mu\nu} = g_{\nu\mu}$. Under these conditions we plug Eq. (4.5) into the Euler-Lagrange equation which yields:

$$g_{\mu\nu} \frac{d^2 x^\nu}{d\sigma^2} = \frac{1}{2} \partial_\mu g_{\nu\kappa} \frac{dx^\kappa}{d\sigma} \frac{dx^\nu}{d\sigma} - \partial_\kappa g_{\mu\nu} \frac{dx^\nu}{d\sigma} \frac{dx^\kappa}{d\sigma}. \tag{4.7}$$

Now we notice that we can rewrite the second term on the right side as:

$$\partial_\kappa g_{\mu\nu} \frac{dx^\nu}{d\sigma} \frac{dx^\kappa}{d\sigma} = \frac{1}{2} \left(\partial_\kappa g_{\mu\nu} + \partial_\nu g_{\mu\kappa} \right) \frac{dx^\nu}{d\sigma} \frac{dx^\kappa}{d\sigma}, \tag{4.8}$$

and if we substitute Eq. (4.8) into Eq. (4.7) we find instead:

$$g_{\mu\nu} \frac{d^2 x^\nu}{d\sigma^2} = -\frac{1}{2} \left(\partial_\kappa g_{\mu\nu} + \partial_\nu g_{\mu\kappa} - \partial_\mu g_{\nu\kappa} \right) \frac{dx^\nu}{d\sigma} \frac{dx^\kappa}{d\sigma}. \tag{4.9}$$

We now multiply both sides of Eq. (4.9) with the contravariant inverse $g^{\lambda\mu}$ along with $(1/L)^2 = (d\sigma/d\tau)^2$ in order to trade derivatives with respect to σ with derivatives with respect to τ. Using Eq. (4.6) meanwhile changing indices we then find:

$$\frac{d^2 x^\mu}{d\tau^2} = -\frac{1}{2} g^{\mu\lambda} \left(\partial_\kappa g_{\lambda\nu} + \partial_\nu g_{\lambda\kappa} - \partial_\lambda g_{\nu\kappa} \right) \frac{dx^\nu}{d\tau} \frac{dx^\kappa}{d\tau}. \tag{4.10}$$

Showing that the action functional in Eq. (4.2) produces the same equations of motion is a bit more difficult. Plugging the Lagrangian in Eq. (4.3) into the Euler-Lagrange we find that

$$\frac{1}{2} \frac{1}{L} \partial_\mu g_{\nu\kappa} \frac{dx^\nu}{d\sigma} \frac{dx^\kappa}{d\sigma} - \frac{d}{d\sigma} \left(\frac{1}{L} g_{\mu\nu} \frac{dx^\nu}{d\sigma} \right) = 0. \tag{4.11}$$

Now, $1/L = d\sigma/d\tau$ so multiplying Eq. (4.11) with $d\sigma/d\tau$ gives us:

$$\frac{1}{2} \partial_\mu g_{\nu\kappa} \frac{dx^\nu}{d\tau} \frac{dx^\kappa}{d\tau} - \frac{d}{d\tau} \left(g_{\mu\nu} \frac{dx^\nu}{d\tau} \right) = 0. \tag{4.12}$$

If we expand the second term we see that

$$g_{\mu\nu} \frac{d^2 x^\nu}{d\tau^2} = \frac{1}{2} \partial_\mu g_{\nu\kappa} \frac{dx^\kappa}{d\tau} \frac{dx^\nu}{d\tau} - \partial_\kappa g_{\mu\nu} \frac{dx^\nu}{d\tau} \frac{dx^\kappa}{d\tau}, \tag{4.13}$$

which is exactly the same as Eq. (4.7) if we multiply both sides by $L^2 = (d\tau/d\sigma)^2$ to change derivatives, and derivation of Eq. (4.10) now follows naturally according to Eq. (4.8) — Eq. (4.10). Q.E.D.

We have derived the equations of motion, Eq. (4.10), for a particle in spacetime and we now define the **Christoffel symbols** as:

$$\Gamma^{\mu}{}_{\nu\kappa} \equiv \frac{1}{2} g^{\mu\lambda} \left(\partial_\kappa g_{\lambda\nu} + \partial_\nu g_{\lambda\kappa} - \partial_\lambda g_{\nu\kappa} \right), \tag{4.14}$$

which allows us to rewrite the equations of motion as:

$$\frac{d^2 x^\mu}{d\tau^2} = -\Gamma^{\mu}{}_{\nu\kappa} \frac{dx^\nu}{d\tau} \frac{dx^\kappa}{d\tau}, \tag{4.15}$$

and so we have arrived at the geodesic equation. Unlike the metric $g_{\mu\nu}$, the Christoffel symbols are not tensors because they do not transform like tensors under a change of coordinates. The Christoffel symbols transform in such a way that it is always possible to find coordinate systems in which they become zero at any given point, Eq. (4.15) then reduces to the equation for a free particle. In other words this is a form of the principle of equivalence.

We will never actually have to use the geodesic equation directly in this thesis. Instead we will see that the relevant equations will be derivable by means of looking for constants of the motion. Regardless it is illuminating to see what the equations of motion look like in the general case, which is why the geodesic equation has been derived here.

4.2 The Radial Equation of the Schwarzschild Geometry

The Schwarzschild metric is an exact solution to the Einstein vacuum equation given by the lineelement:

$$ds^2 = -\left(1 - \frac{2M}{r}\right) dt^2 + \left(1 - \frac{2M}{r}\right)^{-1} dr^2 + r^2 \left(d\theta^2 + \sin^2\theta \, d\phi^2\right), \tag{4.16}$$

which written as a matrix consequently becomes:

$$g_{\mu\nu} = \begin{pmatrix} -(1-2M/r) & 0 & 0 & 0 \\ 0 & (1-2M/r)^{-1} & 0 & 0 \\ 0 & 0 & r^2 & 0 \\ 0 & 0 & 0 & r^2 \sin^2\theta \end{pmatrix}. \tag{4.17}$$

The Schwarzschild metric has a few interesting properties, it is clear that it is independent of t and ϕ and hence there exist **Killing vectors** $\xi^\mu = (1,0,0,0)^\intercal$ and $\eta^\mu = (0,0,0,1)^\intercal$ which both lie along directions in which the metric in Eq. (4.17) doesn't change*. We define the four-vector u^μ as

$$u^\mu \equiv \frac{dx^\mu}{d\tau}, \tag{4.18}$$

where we let indices run over the coordinates (t, r, θ, ϕ) and τ is the proper time. Now, since the metric is independent of t, forming the scalar product between ξ^μ and $u_\mu = g_{\mu\nu}u^\nu$ gives us the quantity:

$$e = -g_{\mu\nu}\xi^\mu u^\nu = \left(1 - \frac{2M}{r}\right)\frac{dt}{d\tau}, \tag{4.19}$$

where the constant e is the energy per unit rest mass. Similarly since the metric is independent of ϕ we form the constant ℓ according to:

$$\ell = g_{\mu\nu}\eta^\mu u^\nu = r^2 \sin^2\theta \frac{d\phi}{d\tau}, \tag{4.20}$$

which is the angular momentum per unit rest mass. As in Newtonian mechanics, conservation of angular momentum implies that the orbits lie in a plane, hence we can set $\theta = \pi/2$ and $u^\theta = 0$, furthermore the normalization of the four velocity vector gives us:

$$u_\mu u^\mu = g_{\mu\nu}u^\mu u^\nu = -1, \tag{4.21}$$

where the last equality follows from $ds^2 = g_{\mu\nu}dx^\mu dx^\nu = -d\tau^2$. Evidently we can now write out Eq. (4.21) for the Schwarzschild metric, assuming motion in the equatorial plane, and consequently arrive at:

$$-\left(1 - \frac{2M}{r}\right)\left(u^t\right)^2 + \left(1 - \frac{2M}{r}\right)^{-1}(u^r)^2 + r^2\left(u^\phi\right)^2 = -1. \tag{4.22}$$

*There are actually four Killing vectors for the Schwarzschild metric since it is invariant under time translations and rotations. But we will only need two of them for our purpose.

Now we exploit the relations in Eq. (4.19) and Eq. (4.20) and rewrite Eq. (4.22):

$$-\left(1-\frac{2M}{r}\right)^{-1}e^2+\left(1-\frac{2M}{r}\right)^{-1}\left(\frac{dr}{d\tau}\right)^2+\frac{\ell^2}{r^2}=-1, \tag{4.23}$$

and solving this equation for $(e^2-1)/2$ gives us:

$$\frac{e^2-1}{2}=\left(\frac{dr}{d\tau}\right)^2+V_{\text{eff}}(r), \tag{4.24}$$

which is the radial equation in the Schwarzschild geometry with the corresponding effective potential:

$$V_{\text{eff}}(r)=\frac{\ell^2}{2r^2}-\frac{M}{r}-\frac{M\ell^2}{r^3}. \tag{4.25}$$

Thus, a system of four coupled differential equations in four variables has, with the help of three constants of the motion, been reduced to a single differential equation in one variable.

Now recall the Schwarzschild metric in Eq. (4.16). As $r\to 2M$, the lineelement approaches a singularity. Physically there is nothing special occuring locally in spacetime. Instead it turns out that this is a coordinate singularity, and in order to solve this problem we transform the time coordinate according to:

$$t=v-r-2M\ln\left|\frac{r}{2M}-1\right|. \tag{4.26}$$

The differential dt^2 then takes the following form:

$$dt^2=\left(dv-\frac{dr}{1-\frac{2M}{r}}\right)^2=dv^2-\frac{2dvdr}{1-\frac{2M}{r}}+\frac{dr^2}{\left(1-\frac{2M}{r}\right)^2}, \tag{4.27}$$

which consequently transforms Eq. (4.16) into:

$$ds^2=-\left(1-\frac{2M}{r}\right)dv^2+2dvdr+r^2d\Omega, \tag{4.28}$$

which are the **Eddington-Finkelstein coordinates** with the corresponding off-diagonal metric tensor:

$$g_{\mu\nu}=\begin{pmatrix}-(1-2M/r) & 1 & 0 & 0\\ 1 & 0 & 0 & 0\\ 0 & 0 & r^2 & 0\\ 0 & 0 & 0 & r^2\sin^2\theta\end{pmatrix}. \tag{4.29}$$

From Eq. (4.28) it is clear that the singularity which arose in the Schwarzschild coordinates is now nonexistent. Only one singularity is now left and it can be found at $r=0$ which is the actual singularity of the black hole where the curvature of spacetime is infinite.

The radius $r=2M$ is however of significant interest as it defines the null three-surface of a black hole called the event horizon. Here the Killing vector ξ^μ becomes lightlike as $\xi_\mu\xi^\mu=0$ for $r=2M$. At a radius $r<2M$ no light rays can escape the black hole and outside the event horizon at a radius $r>2M$ there are light rays which can take information to distant observers. We shall study the event horizon of black holes more thoroughly later on.

Having derived the effective potential for motion in the Schwarzschild geometry in Eq. (4.25); we now move on to explore the properties of motion in the equatorial plane by looking for circular orbits. We begin by looking for extrema of the effective potential, and to this end we resort to its derivative:

$$\frac{dV_{\text{eff}}}{dr}=\frac{M}{r^2}+\frac{3M\ell^2}{r^4}-\frac{\ell^2}{r^3}, \tag{4.30}$$

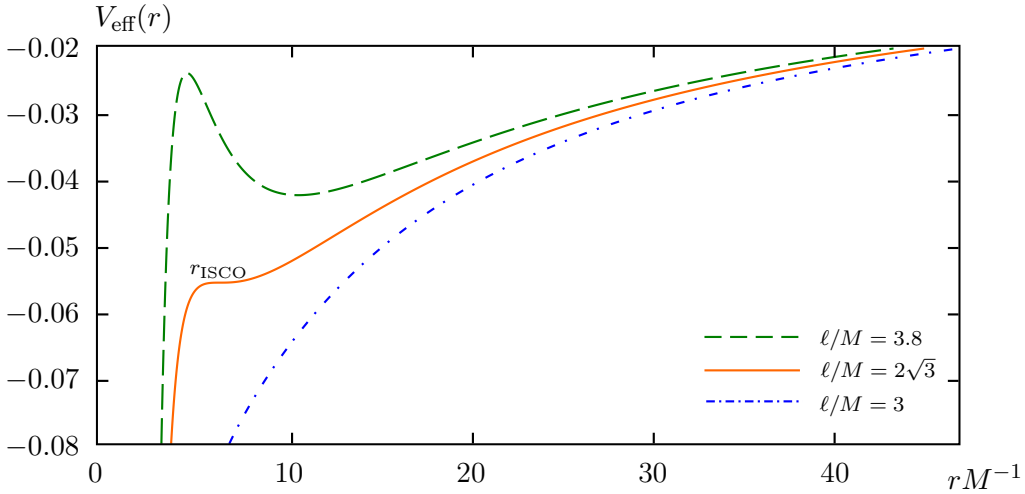

Figure 4.1: Relativistic effective potentials for various values of ℓ/M with $M = 1$. The dashed curve represents an effective potential with two extremas. The middle full drawn curve represent the effective potential for r_{ISCO}. The dashed and dotted line on the other hand represent an effective potential which lacks a stable orbit.

and the solutions for $dV_{\text{eff}}/dr = 0$ is given by:

$$r = \frac{\ell^2}{2M} \pm \left[\left(\frac{\ell^2}{2M} \right)^2 - 3\ell^2 \right]^{1/2}. \tag{4.31}$$

From Eq. (4.31) it is obvious that the inequality $\ell^2 \geq 12M^2$ must hold; if it doesn't the solution to the derivative of the effective potential has imaginary roots, and consequently we would be unable to find any stable orbits. Upon inspection of Eq. (4.31) we see that the lowest possible value for r occurs when $\ell^2 = 12M^2$, the square root then becomes zero and we find:

$$r_{\text{ISCO}} = 6M, \tag{4.32}$$

which is the innermost stable circular orbit (ISCO), for the Schwarzschild geometry. Three

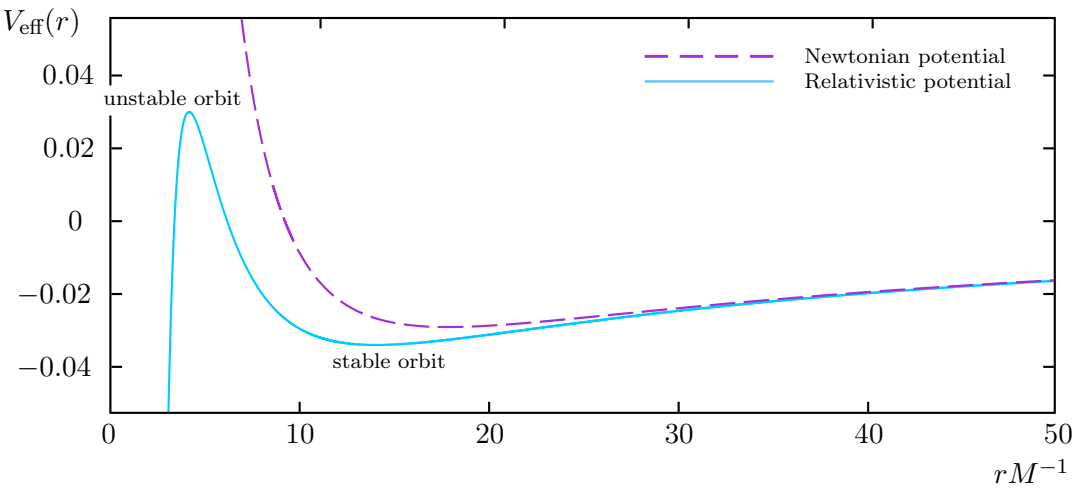

Figure 4.2: A comparison between the effective potentials arising in classical mechanics and general relativity for $\ell/M = 4.2$ and $M = 1$. The dashed line portrays the classical case with a "barrier" where the effective potential goes to infinity as r goes to zero. In contrast to the relatvistic case (full drawn line), where the "barrier" becomes finite as a consequence of a correction term involving r^{-3}.

cases each for different values of ℓ/M are shown in Fig. 4.1, and a relation to the classical potential is given in Fig. 4.2.

4.3 Properties of the Kerr Geometry

For a rotating black hole with mass M, angular momentum J and the coordinates (t, r, θ, ϕ) the line element of spacetime, in geometrized units with $G = c = 1$, is given by:

$$\begin{aligned} ds^2 = &-\left(1 - \frac{2Mr}{\rho^2}\right) dt^2 - \frac{4Mar\sin^2\theta}{\rho^2} d\phi dt + \frac{\rho^2}{\Delta} dr^2 + \rho^2 d\theta^2 \\ &+ \left(r^2 + a^2 + \frac{2Mra^2\sin^2\theta}{\rho^2}\right)\sin^2\theta\, d\phi^2, \end{aligned} \tag{4.33}$$

where $\rho^2 \equiv r^2 + a^2\cos^2\theta$, $\Delta \equiv r^2 - 2Mr + a^2$ and $a \equiv J/M$.

From the line element it is obvious that the corresponding tensor is not on diagonal form as a consequence of the presence of a term involving $d\phi dt$. By inspection we see that the tensor corresponding to the line element in Eq. (4.33) must be given by:

$$g_{\mu\nu} = \begin{pmatrix} -\left(1 - \frac{2Mr}{\rho^2}\right) & 0 & 0 & -\frac{2Mar\sin^2\theta}{\rho^2} \\ 0 & \frac{\rho^2}{\Delta} & 0 & 0 \\ 0 & 0 & \rho^2 & 0 \\ -\frac{2Mar\sin^2\theta}{\rho^2} & 0 & 0 & \left(r^2 + a^2 + \frac{2Mra^2\sin^2\theta}{\rho^2}\right)\sin^2\theta \end{pmatrix}, \tag{4.34}$$

with off-diagonal elements $g_{t\phi} = g_{\phi t}$. The metric described here is a solution of the vacuum Einstein equation and we shall explore some of its most important properties.

What distinguishes the Kerr geometry from the Schwarzschild geometry is rotation. The Kerr geometry involves the angular momentum J meanwhile the Schwarzschild geometry assumes that there is no rotation involved. So we ought to expect that when we set the Kerr parameter $a = 0$, the Kerr geometry should reduce to the Schwarzschild geometry. Under this circumstance the parameters $\rho^2 = r^2$ and $\Delta = r^2 - 2Mr$, so evidently Eq. (4.33) turns into

$$ds^2 = -\left(1 - \frac{2M}{r}\right) dt^2 + \left(1 - \frac{2M}{r}\right)^{-1} dr^2 + r^2\left(d\theta^2 + \sin^2\theta\, d\phi^2\right), \tag{4.35}$$

which is the Schwarzschild geometry as we would expect.

From the Kerr metric it also follows that it is independent of t and hence stationary, furthermore the metric is independent of ϕ so there exist Killing vectors $\xi^\mu = (1, 0, 0, 0)^\intercal$ and $\eta^\mu = (0, 0, 0, 1)^\intercal$.

Further investigation of Eq. (4.33) reveals singularities when ρ and Δ vanishes. The singularity for $\rho = 0$ arises when $r = 0$ and $\theta = \pi/2$, which corresponds to a real, physical singularity and is the generalization of the physical singularity in the Schwarzschild metric. Evidently the two coincide when $a = 0$, that is to say for zero angular momentum, as expected.

For $\Delta = 0$ we have the solution:

$$r_\pm = M \pm \left(M^2 - a^2\right)^{1/2}, \tag{4.36}$$

Here, $r = r_+$ defines the event horizon in the Kerr geometry, and unless $a \leq M$ the event horizon does not exist. As we saw for the Schwarzschild metric this is a coordinate singularity*, furthermore it is clear that under the condition $a = 0$, Eq. (4.36) reduces to $r_+ = 2M$, that is to say at the event horizon in the Schwarzschild geometry.

*As for the Schwarzschild metric it is possible to make a change of coordinates which effectively rids us of this singularity, however we shall not do so here.

Eq. (4.36) thus defines the generalization of the event horizon we mentioned for the Schwarzschild metric. Evidently then the event horizon ranges from $r = 2M$ when $a = 0$ to $r = M$ when $a = M$ for extremal black holes. With other words as the angular momentum per mass of black holes increases, the radius of the event horizon gets smaller.

From Eq. (4.36) we also find that the Kerr parameter $a \leq M$, a limitation which does not apply to other astronomical objects such as stars. This peculiarity will be one of the main topics of Chapter 5.

In general, the orbits of particles in the Kerr geometry are not confined to a plane like they are in the Schwarzschild geometry, because we no longer have spherical symmetry. But, the metric is still axisymmetric so there exist orbits in the equatorial plane, and such orbits are especially interesting to us since the accretion disk mentioned earlier lies close to the equatorial plane.* We will restrict our attention to such orbits and for the equatorial plane we then have that $\theta = \pi/2$, and consequently $u^\theta = 0$. Following this discussion the Kerr geometry in Eq. (4.33) reduces to:

$$ds^2 = -\left(1 - \frac{2M}{r}\right) dt^2 - \frac{4Ma}{r} d\phi dt + \frac{r^2}{\Delta} dr^2 + \left(r^2 + a^2 + \frac{2Ma^2}{r}\right) d\phi^2. \tag{4.37}$$

Now, since the Kerr metric is independent of t and ϕ there exist conserved quantities:

$$e = -g_{\mu\nu}\xi^\mu u^\nu \quad \text{and} \quad \ell = g_{\mu\nu}\eta^\mu u^\nu, \tag{4.38}$$

where e is the energy per unit rest mass, ℓ is the angular momentum per unit rest mass, ξ^μ and η^μ are our Killing vectors found earlier. Upon inspection of the Kerr metric we see that both of the quantities in Eq. (4.38) are linear combinations of u^t and u^ϕ according to:

$$-e = g_{tt}u^t + g_{t\phi}u^\phi, \tag{4.39}$$

$$\ell = g_{\phi t}u^t + g_{\phi\phi}u^\phi. \tag{4.40}$$

Which we invert to solve for u^t and u^ϕ:

$$u^t = -\frac{1}{\Delta}\left(\ell g_{t\phi} - e g_{\phi\phi}\right), \tag{4.41}$$

$$u^\phi = -\frac{1}{\Delta}\left(\ell g_{tt} + e g_{\phi t}\right). \tag{4.42}$$

Or written out explicitly:

$$\frac{dt}{d\tau} = \frac{1}{\Delta}\left[\left(r^2 + a^2 + \frac{2Ma^2}{r}\right) e - \frac{2Ma}{r}\ell\right], \tag{4.43}$$

$$\frac{d\phi}{d\tau} = \frac{1}{\Delta}\left[\left(1 - \frac{2M}{r}\right)\ell + \frac{2Ma}{r}e\right]. \tag{4.44}$$

Now we apply the normalization condition $g_{\mu\nu}u^\mu u^\nu = -1$ and after a lengthy calculation we arrive at the radial equation for equatorial motion:

$$\frac{e^2 - 1}{2} = \left(\frac{dr}{d\tau}\right)^2 + V_{\text{eff}}(r), \tag{4.45}$$

where $V_{\text{eff}}(r)$ is the effective potential given by:

$$V_{\text{eff}}(r) = \frac{\ell^2 - a^2(e^2 - 1)}{2r^2} - \frac{M\left(\ell - ae\right)^2}{r^3} - \frac{M}{r}, \tag{4.46}$$

which governs the radial motion. Much of the remainder of this thesis will be based on this equation.

*For the general case see Carter [18].

Chapter 5

Evolution of the Angular Momentum of Black Holes

In this chapter we will explore and derive the solutions to the radial equation for geodesics in the equatorial plane of Kerr black holes. These solutions will be derived analytically without any computer aided help. This is accomplished by manipulation of the radial equation, and in this manner the equation system reduces to a much simpler form.

We then move on to study the accretion of matter from a disk of gas in orbit around a black hole. From r_{ISCO} particles are being dumped directly down into the black hole, increasing both its mass and angular momentum per mass squared. The solutions found in section 5.1 are then used in deriving Eq. (3.30) which gives the angular momentum per mass squared as a function of the mass of the black hole. Following this we discuss disk-accretion for black holes near the extremal limit, and it will there be argued that photon emission from the surface of the accretion disk becomes an essential part in the analysis of the evolution of the angular momentum per mass squared in order to investigate whether cosmic censorship is violated or not.

Finally we investigate how the area of the event horizon changes as the angular momentum per mass squared increases and mass is accreted.

5.1 Solutions to the Radial Equation of the Kerr Metric

In chapter 4 we derived the radial equation for the Kerr metric, and we now wish to find analytic solutions to this equation. In principle we may imagine that values for r_{ISCO} are known and that the angular momentum per mass squared $\tilde{a}$ is an unknown which we wish to solve for. Furthermore in the next section we will study how disk-accretion affects $\tilde{a}$ as black holes accrete matter and in order to do so expressions for the angular momentum per unit rest mass of particles ℓ and the energy per unit rest mass of particles e will be valuable for us. So, with the ultimate goal of solving Eq. (4.45), for e, ℓ and $\tilde{a}$ in terms of r_{ISCO}, we now define the potential $V(r)$ as:

$$\begin{aligned} V(r) &\equiv -2r^2\left(V_{\text{eff}}(r) - \frac{e^2-1}{2}\right) \\ &= (r^2+a^2)(e^2-1) + \frac{2M(\ell-ae)^2}{r} + 2Mr - \ell^2, \end{aligned} \tag{5.1}$$

where $r > 0$ and here r_{ISCO} is the value of r for which we get the innermost stable, or marginally stable, orbit with constant r. From this potential we now intend to derive Eqs. (3.28). Note here that for r_{ISCO} it necessarily follows that $dr/d\tau = 0$ and for particles to remain in circular orbit the conditions $V(r) = 0$ and $V'(r) = 0$ must hold. Furthermore

for a stable orbit we have the condition $V''(r) > 0$, and since r_{ISCO} is the orbit which is on the verge of being unstable we find that this condition becomes an equality: $V''(r) = 0$. Hence we have a nonlinear system of three equations in three unknowns to solve for.

The derivative of $V(r)$ is given by:

$$V'(r) = 2r(e^2 - 1) - \frac{2M(\ell - ae)^2}{r^2} + 2M. \tag{5.2}$$

Eq. (5.1) and Eq. (5.2) can be used to solve for e and ℓ in terms of r, M and a using computer algebraic methods (see Bardeen, Press & Teukolsky [16]). Note that we do not intend to derive all the results from this paper, but only the ones we need.

As we now shall see there is a simple way of exploiting the similar structure of these equations, which simplifies matters significantly and allows us to perform the calculations without a computer. In each of these equations there is a term involving $(\ell - ae)^2$, by multiplying the derivative of the potential by r, which we can do since r is finite* and $V'(r) = 0$, and adding these two equations together we can eliminate this term and arrive at a much simpler expression:

$$V(r) + rV'(r) = (3r^2 + a^2)(e^2 - 1) + 4Mr - \ell^2. \tag{5.3}$$

We know from before that the second derivative $V''(r) = 0$ for the innermost stable circular orbit in the equatorial plane, therefore we can differentiate Eq. (5.3) a second time since

$$\frac{d}{dr}\left[V(r) + rV'(r)\right] = 2V'(r) + rV''(r), \tag{5.4}$$

only contains the first and second derivative.

Our problem now reduces to solving the equation system:

$$V(r) = V(r) + rV'(r) + 2V'(r) + rV''(r) = 0. \tag{5.5}$$

Note that as soon as we have imposed the condition $V''(r) = 0$ the radius r must necessarily be r_{ISCO}. Therefore, from now on whenever we refer to r it should be clear that we are *always* referring to r_{ISCO}. With this in mind we find that Eq. (5.3) reduces to:

$$\frac{d}{dr}\left[V(r) + rV'(r)\right] = 6r(e^2 - 1) + 4M, \tag{5.6}$$

and from this it follows that

$$e = \left(1 - \frac{2M}{3r}\right)^{1/2}, \tag{5.7}$$

where we have neglected the negative solution.

Having found a simple expression for the energy in terms of r, we now move on to use this solution with the purpose of finding similar solutions for ℓ and a. Now, differentiating Eq. (5.2) a second time we find:

$$V''(r) = 2(e^2 - 1) + \frac{4M(\ell - ae)^2}{r^3}. \tag{5.8}$$

Plugging in our newly found expression for e and using $V''(r) = 0$, the equation turns into:

$$\frac{r^2}{3} = \left[\ell - a\left(1 - \frac{2M}{3r}\right)^{1/2}\right]^2, \tag{5.9}$$

*In principle $r \to \infty$ for particles far away from the black hole, but this won't cause us any trouble for obvious reasons.

and solving this equation for ℓ we arrive at:

$$\ell = a\left(1 - \frac{2M}{3r}\right)^{1/2} \pm \frac{r}{3^{1/2}}. \tag{5.10}$$

Combining Eq. (5.3) and Eq. (5.7) we find a second equation in ℓ and a:

$$-\frac{2M}{3r}\left(3r^2 + a^2\right) - \ell^2 + 4Mr = 0, \tag{5.11}$$

which after some simplification can be turned into:

$$\ell^2 = 2M\left(r - \frac{a^2}{3r}\right). \tag{5.12}$$

We now plug in our solution for ℓ which we found in Eq. (5.10) which turns the equation into:

$$\left[a\left(1 - \frac{2M}{3r}\right)^{1/2} \pm \frac{r}{3^{1/2}}\right]^2 = 2M\left(r - \frac{a^2}{3r}\right), \tag{5.13}$$

and thus we have eliminated the dependence on ℓ and move on to solve this expression for a. It turns out that after expanding the left side and combining all terms in a^2, two terms cancel resulting in:

$$a^2 \pm \frac{2ar}{3^{1/2}}\left(1 - \frac{2M}{3r}\right)^{1/2} = 2Mr - \frac{r^2}{3}. \tag{5.14}$$

After some elementary algebra additional terms cancel and we find ourselves dealing with the expression:

$$\left[a \pm \frac{r}{3^{1/2}}\left(1 - \frac{2M}{3r}\right)^{1/2}\right]^2 = \frac{16Mr}{9}, \tag{5.15}$$

which after solving for a simplifies to:

$$a = \pm\frac{4M^{1/2}r^{1/2}}{3} \mp \frac{r}{3^{1/2}}\left(1 - \frac{2M}{3r}\right)^{1/2} \tag{5.16}$$

We now define $\tilde{a} \equiv a/M$ and transform Eq. (5.16) into:

$$\tilde{a} = \pm\frac{4r^{1/2}}{3M^{1/2}} \mp \frac{r}{3^{1/2}M}\left(1 - \frac{2M}{3r}\right)^{1/2}, \tag{5.17}$$

which after some further manipulation gives us:

$$\tilde{a} = \pm\frac{1}{3}\left(\frac{r}{M}\right)^{1/2}\left[4 \mp \left(\frac{3r}{M} - 2\right)^{1/2}\right], \tag{5.18}$$

where the upper signs refer to corotation and the lower signs refer to counterrotation.

Finally we seek an expression which gives ℓ in terms of r, which at this point is a simple matter considering that we have already derived expressions for $\tilde{a}$ and e. To accomplish this task recall Eq. (5.10) which we solved for ℓ. Substituting $a = \tilde{a}M$ in this equation (taking the upper sign) yields:

$$\ell = \frac{1}{3}r^{1/2}M^{1/2}\left[1 - \frac{2M}{3r}\right]^{1/2}\left[4 - \left(\frac{3r}{M} - 2\right)^{1/2}\right] + \frac{r}{3^{1/2}}. \tag{5.19}$$

The expression can be simplified somewhat if we notice that the first square root can be

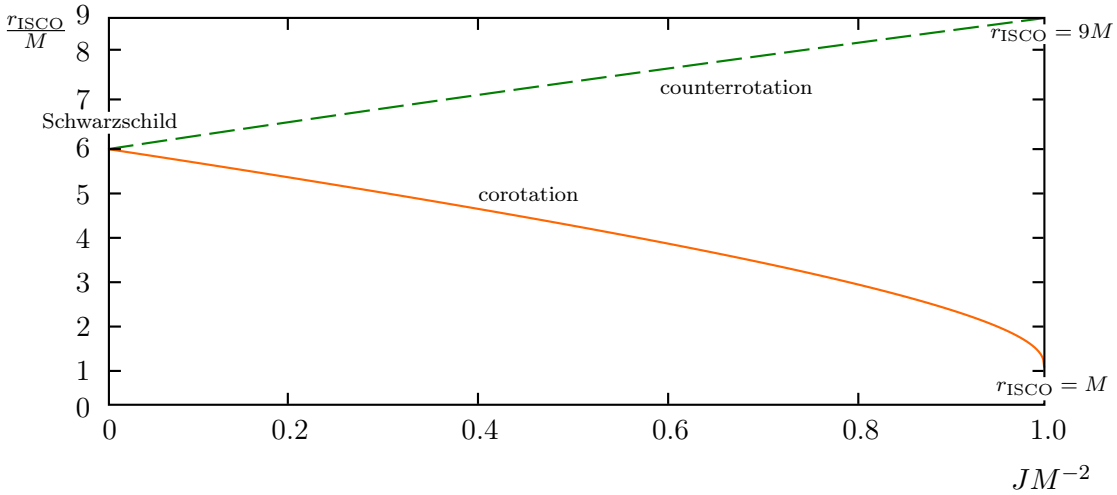

Figure 5.1: The innermost stable circular orbits confined to the equatorial plane for a black hole in the Kerr geometry described by the Boyer-Lindquist radius $r_{\rm ISCO}$ and the angular momentum per mass squared $\tilde{a}$ of the black hole. The lower curve represents $r_{\rm ISCO}$ for a particle in corotation with the black hole meanwhile the dashed line describes $r_{\rm ISCO}$ for counterrotation.

rewritten according to:

$$\ell = \frac{1}{3^{3/2}}\left\{M\left[\frac{3r}{M}-2\right]^{1/2}\left[4-\left(\frac{3r}{M}-2\right)^{1/2}\right]+3r\right\}, \tag{5.20}$$

which upon further simplification turns into:

$$\ell = \frac{2M}{3^{3/2}}\left[1+2\left(\frac{3r}{M}-2\right)^{1/2}\right]. \tag{5.21}$$

We have now derived three expressions for e, ℓ and $\tilde{a}$, in Eq. (5.7), Eq. (5.18) and Eq. (5.21). Finally we define $z \equiv r_{\rm ISCO}/M$ which turns the equations into:

$$e(z) = \left(1-\frac{2}{3z}\right)^{1/2}, \tag{5.22a}$$

$$\ell(z,M) = \frac{2M}{3^{3/2}}\left[1+2(3z-2)^{1/2}\right], \tag{5.22b}$$

$$\tilde{a}(z) = \frac{1}{3}z^{1/2}\left[4-(3z-2)^{1/2}\right], \tag{5.22c}$$

which are exactly the equations in Eqs. (3.28) and hence we are done. Q.E.D.

Finally we mention that z can be solved for as a function of $\tilde{a}$ giving the solutions (see Bardeen, Press and Teukolsky [16]):

$$\begin{aligned} z(\tilde{a}) &= 3 + w_2 \mp \left[(3-w_1)(3+w_1+2w_2)\right]^{1/2} \\ w_1 &\equiv 1 + \left(1-\tilde{a}^2\right)^{1/3}\left[(1+\tilde{a})^{1/3}+(1-\tilde{a})^{1/3}\right] \\ w_2 &\equiv \left(3\tilde{a}+w_1^2\right)^{1/3}, \end{aligned} \tag{5.23}$$

where $z(a) \equiv r_{\rm ISCO}/M$ is called the Boyer-Lindquist radius, the upper sign refers to corotation and the lower sign refers to counterrotation. The general behavior of Eq. (5.23) is shown in Fig. 5.1.

5.2 Disk-accretion Onto Black Holes

Let us consider an accretion disk of gas located in the equatorial plane of a black hole. Suppose now that from the innermost stable circular orbit, gas is being dumped into the black hole. Under this circumstance a gas particle will carry into it an energy per unit rest mass e and an angular momentum per unit rest mass ℓ, corresponding to the values for the last stable circular orbit and given by Eqs. (5.22) which we just derived. We will ignore all other stress-energy such as photon emission from the surface of the disk and later on, see section 5.3, resort to a discussion on what complications such an effect has on the angular momentum per mass squared as it evolves with accretion.

As more gas is being accreted onto the black hole the properties of r_{ISCO} must change accordingly to compensate for the increase in angular momentum and mass of the black hole analogously to what we discovered in the previous section. Thus, the accretion of a rest mass ΔM_0 can be related to the change in the mass ΔM and the angular momentum ΔJ of the black hole (see Thorne, [17]):

$$\Delta M = e(z)\Delta M_0 \quad \text{and} \quad \Delta J = \ell(z, M)\Delta M_0. \tag{5.24}$$

We found expressions for the energy per unit rest mass e, the angular momentum per unit rest mass ℓ and the angular momentum per mass squared $\tilde{a}$ of black holes in the previous section. It turns out to be of great interest to know how the angular momentum per mass squared of black holes evolves as a function of their mass when particles fall in as soft rain from the accretion disk at r_{ISCO}. We now claim that the variation of z can be related to the accreted mass M by the expression:

$$\frac{z}{z_1} = \left(\frac{M_1}{M}\right)^2, \tag{5.25}$$

where M_1 and z_1 are the initial values of the black hole determined from the condition $\tilde{a} = 0$ where we assume* for definiteness that the initial conditions are such that they are described by the Schwarzschild solution.

To prove that the solution in Eq. (5.25) indeed holds we notice that from Eq. (5.24) we have:

$$\frac{d\tilde{a}}{dM} \equiv \frac{d\left(J/M^2\right)}{dM} = \frac{1}{M^2}\frac{\ell(z, M)}{e(z)} - \frac{2}{M}\tilde{a}. \tag{5.26}$$

Using the chain rule to rewrite this equation we find instead:

$$M\frac{dz}{dM}\frac{d\tilde{a}}{dz} = \frac{1}{M}\frac{\ell(z, M)}{e(z)} - 2\tilde{a}. \tag{5.27}$$

After substitution of Eqs. (5.22) it is possible to find a common factor on both sides by rewriting all terms on a common denominator which ultimately yields a separable differential equation with the solution:

$$z = \frac{\mathcal{C}}{M^2}, \tag{5.28}$$

with a constant $\mathcal{C}$ determined from the initial conditions $z = z_1$ and $M = M_1$ which brings us to the final form:

$$\frac{z}{z_1} = \left(\frac{M_1}{M}\right)^2, \tag{5.29}$$

which is exactly the same as Eq. (5.25). Q.E.D.

*It is possible to make modifications to the equations to allow for initial values of $\tilde{a}$ other than zero, these cases are however not especially illuminating in our case which is why we assume that accretion always starts from $\tilde{a} = 0$.

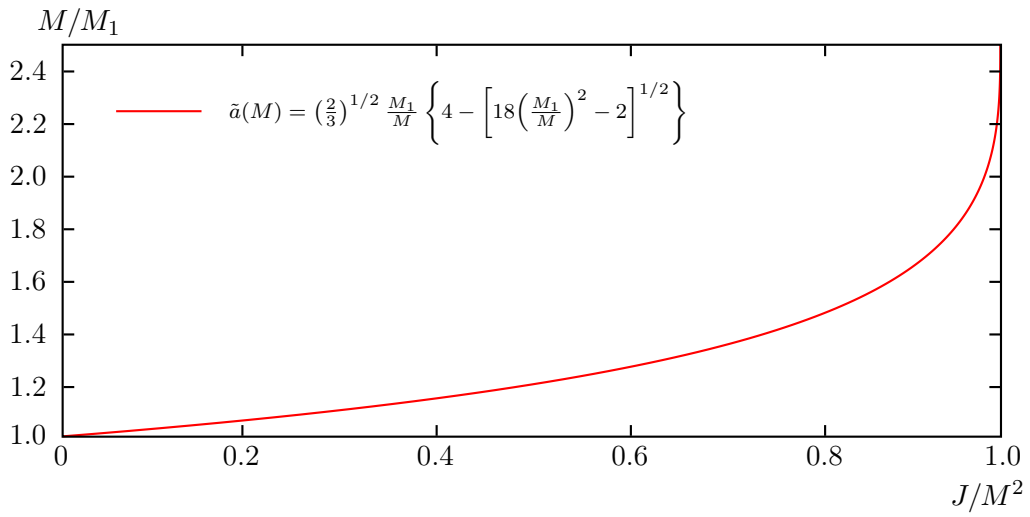

Figure 5.2: The evolution of the angular momentum per mass squared starting from a Schwarzschild black hole. The black hole accretes matter from gas located near the black hole at r_{ISCO}, causing the mass M and the angular momentum J of the black hole to increase. The angular momentum per mass squared $\tilde{a} = 1$ for $M/M_1 = 6^{1/2}$.

We are looking for an expression which gives us the behavior of $\tilde{a}$ as a function of M. Using the relation between z and M, and the fact that $z_1 = 6$ for the Schwarzschild solution with the initial condition $\tilde{a} = 0$, we can rewrite Eq. (5.22c) to give us:

$$\tilde{a}(M) = \left(\frac{2}{3}\right)^{1/2} \frac{M_1}{M} \left\{4 - \left[18\left(\frac{M_1}{M}\right)^2 - 2\right]^{1/2}\right\}, \tag{5.30}$$

which is Eq. (3.30). The general behavior of Eq. (5.30) over values $M/M_1 \leq 6^{1/2}$ is portrayed in Fig. 5.2, the equation is discussed more thoroughly in the next section.

There is another differential equation arising from Eq. (5.24) in terms of the rest mass accreted:

$$\frac{dM}{dM_0} = e(z), \tag{5.31}$$

the equation is separable, and using Eq. (5.25) to eliminate z we find that the solution is given by:

$$M_0 = \int dM \left(\frac{3M_1}{9M_1^2 - M^2}\right) + \mathcal{C} = 3M_1 \arcsin\left(\frac{M}{3M_1}\right) + \mathcal{C}. \tag{5.32}$$

The constant of integration $\mathcal{C}$ can be determined from the initial conditions $M = M_1$ and $M_0 = 0$ which results in the solution:

$$M_0 = 3M_1 \left[\arcsin\left(\frac{M}{3M_1}\right) - \arcsin\left(\frac{1}{3}\right)\right], \tag{5.33}$$

hence we have a way of relating the actual rest mass accreted M_0 to the initial mass M_1 and the mass of the black hole M. Consequently it follows that for $M/M_1 = 6^{1/2}$, $\tilde{a} = 1$ after a rest mass $M_0 = 3M_1 \left[\arcsin\left(2/3\right)^{1/2} - \arcsin\left(1/3\right)\right]$ has been accreted.

In some instances we may be interested in the mass of the black hole in terms of the rest mass accreted. Eq. (5.33) can then be solved for M:

$$\frac{M}{M_1} = 3\sin\left[\frac{M_0}{3M_1} + \arcsin\left(\frac{1}{3}\right)\right], \tag{5.34}$$

which with the aid of some elementary trigonometry can be rewritten as:

$$\frac{M}{M_1} = 2\sqrt{2}\sin\left(\frac{M_0}{3M_1}\right) + \cos\left(\frac{M_0}{3M_1}\right). \tag{5.35}$$

The equations given in Bardeen's paper [12] have now been derived. These are Eqs. (5.22), Eq. (5.29) and Eq. (5.35).*

In this section we have studied only one of the many ways the angular momentum of black holes can actually change meanwhile there are many other processes which have an impact on the angular momentum. There is a particularly interesting phenomenon which can decrease the angular momentum of black holes; a completely different situation from the one we have studied. Suppose that a black hole is being randomly bombarded by particles from all directions of space. Recall Fig. 5.1 which tells us that as the angular momentum per mass squared of black holes increases, r_{ISCO} for corotating particles decreases meanwhile the opposite is true for particles in counterrotation with the black hole. The cross section for counterrotating particles falling into the black hole is thus much greater than the cross section for particles in corotation with the black hole, since there exist stable orbits for corotating particles much further in than for counterrotating particles. From this process the angular momentum of the black hole consequently tends to decrease. The situation is depicted in Fig. 5.3.

Suppose that a particle is falling towards a black hole from infinity, if the particle falls towards it in such a way that it will get caught by the spacetime curvature of the black hole and ultimately fall down it; then it may be more appropriate to refer to the particles as having either positive or negative angular momentum with respect to the black hole rather than saying that the particle is "corotating" or "counterrotating" with the black hole. After all the particle is not traveling along a geodesic which is an orbit of the black hole. The same principle of course still applies, a particle falling towards the black hole in a direction which is against the rotation of the black hole will still be more easily caught than a particle traveling in a direction which is with the rotation of the black hole.

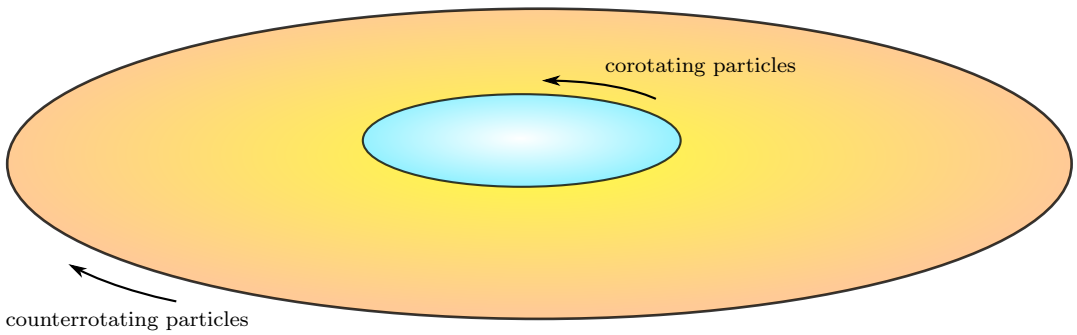

Figure 5.3: The picture portrays the capture zones for a black hole in the equatorial plane which carries a value of $\tilde{a}$ high enough to give a noticeable difference between the capture zones for corotating particles and counterrotating particles. The larger disk portrays the capture zone for counterrotating particles and the smaller disk, embodied within it, portrays the capture zone for particles in corotation with the black hole. Since the black hole carries angular momentum, these capture zones differ noticeably and causes counterrotating particles to be more easily caught by the black hole than corotating particles. The end result is a decrease in angular momentum from such a process of accretion.

*Note that Bardeen's version reduces to Eq. (5.35) if we let $z_1 = 6$.

For more information regarding various processes which can change the angular momentum per mass squared of black holes see Rees, Rufini & Wheeler, [19].

5.3 Accretion for Near Extremal Black Holes

The observant reader may at this point have noticed that Eq. (5.30) behaves in a rather peculiar manner. A basic analysis shows that the domain of the function is $1 \leq M/M_1 \leq 3$,* which consequently means that the range of the function is $0 \leq \tilde{a} \lesssim 1.0887$. In other words, when analyzed mathematically the function seem to imply that it is possible for a black hole, by accretion of matter from r_{ISCO} according to the equations derived in the previous sections, to acquire values of $\tilde{a} > 1$ and in so doing violate cosmic censorship. In his paper [12] Bardeen argued that accretion increases the angular momentum per mass squared until $\tilde{a} = 1$ after which *"further accretion will keep a equal to M"*, it is however perfectly clear that such a conclusion cannot be drawn directly from the behavior of Eq. (5.30), rather this must be a behavior imposed upon the function in order for it not to violate cosmic censorship.

Mathematically, the restriction imposed upon the function by Bardeen makes perfect sense. This can be seen by examining Eq. (5.30) further by investigating how its derivative behaves around $\tilde{a} = 1$. For simplicity we let $M_1 = 1$, the derivative of Eq. (5.30) is then given by:

$$\frac{d\tilde{a}}{dM} = \frac{1}{M^2}\left(\frac{2}{3}\right)^{1/2}\left[\left(\frac{18}{M^2} - 2\right)^{1/2} + \frac{18}{M^2}\left(\frac{18}{M^2} - 2\right)^{-1/2} - 4\right]. \tag{5.36}$$

For $\tilde{a} = 1$ we have that $M/M_1 = 6^{1/2}$ which means that $d\tilde{a}/dM = 0$ when $\tilde{a} = 1$.

Now, since the derivative is zero when $\tilde{a} = 1$ we can disregard what happens with Eq. (5.30) past this value and add a constant function which keeps $\tilde{a} = 1$ for values of $M/M_1 > 6^{1/2}$. In this manner the resulting functions first derivative will still be continuous.

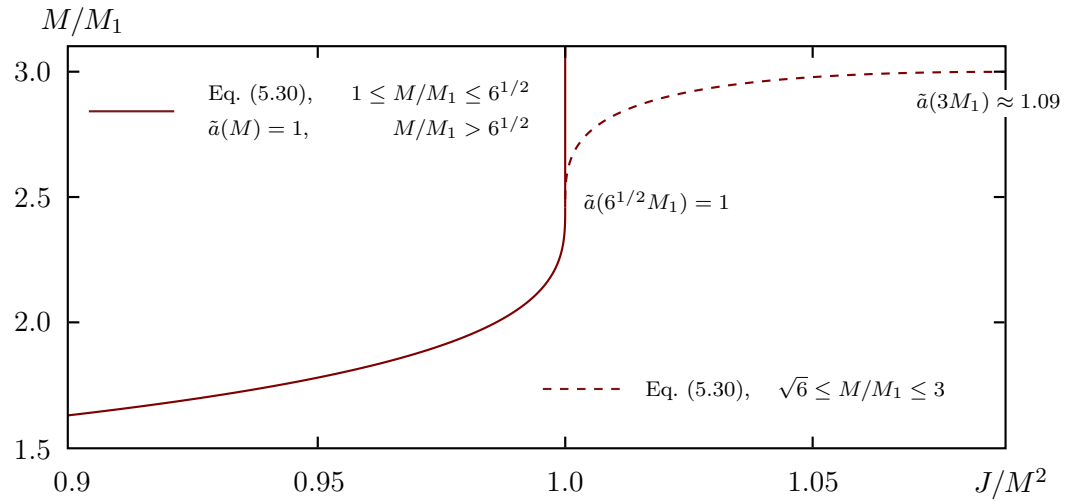

Figure 5.4: Eq. (5.30) is here plotted along with its correction at $\tilde{a} = 1$. This correction prevents a black hole from acquiring an angular momentum per mass squared $\tilde{a} > 1$ as it continuous to accrete matter (full drawn curve). The values for Eq. (5.30) when $M/M_1 > 6^{1/2}$ is also plotted (dashed curve), which shows the peculiar behavior of the function for high values of the angular momentum per mass squared. The function is not defined for values $M/M_1 > 3$.

*Mathematically the function is defined for values $M/M_1 < 1$ but these values are not of any physical interest.

That the restriction imposed upon Eq. (5.30) makes sense mathematically, doesn't necessarily mean that it makes sense physically. Eq. (5.30) for high values of $\tilde{a}$ is shown in Fig. 5.4, and it can here be seen that the unmodified function has a seemingly very strange behavior. The function has a turning point when $\tilde{a} = 1$, after which $\tilde{a}$ begins to increase more and more rapidly as the mass increases, furthermore the function is not even defined for values of $M/M_1 > 3$ which is very strange; we ought to expect that a function which gives the evolution of $\tilde{a}$ as a function of mass allows for black holes to increase their mass indefinitely. In other words we are lead to conclude that something is probably not quite right here, and if the function behaves in such a peculiar manner for high values of $\tilde{a}$, then perhaps we should also question its validity in general.

A few years after Bardeen's paper, Kip Thorne published a paper [17] in response. Thorne modified Bardeen's equation to also account for contributions to the angular momentum per mass squared in the form of photons emitted from the surface of the accretion disk of a black hole. Thorne argued that photons emitted from the disk would travel along null geodesics which either escape to infinity or gets recaptured by the black hole. Some photons will travel along geodesics which are *against* the direction of the spin of the black hole, carrying negative angular momentum, and some will travel along geodesics which are *with* the rotation of the black hole and therefore carry positive angular momentum. Those photons carrying positive angular momentum will then increase $\tilde{a}$ of the black hole, and those which carry negative angular momentum will decrease $\tilde{a}$. Since the capture zone for photons carrying negative angular momentum is larger than the capture zone for photons carrying positive angular momentum*, the result of such contributions is to decrease $\tilde{a}$ of the black hole.

This led Thorne to a differential equation which he solved numerically†. Thorne managed to show that the effect of the photons is to limit the angular momentum per mass squared of black holes to a value $\tilde{a} \approx 0.998$, or in other words, the photons "push" the angular momentum per mass squared away from the extremal limit $\tilde{a} = 1$. Furthermore if black holes start with a very high value close to $\tilde{a} = 1$ the effect of the photons is to spin black holes down, *reducing* $\tilde{a}$ to its limiting value $\tilde{a} \approx 0.998$. Thorne's solution allow black holes to accrete matter indefinitely without violating cosmic censorship, consequently solving the issues stated above for Bardeen's equation.

It turns out that the equation derived by Bardeen is in good agreement with Thorne's solution for values of $\tilde{a} < 0.9$, above this value the effect of photons become significant and Bardeen's equation begins to deviate from Thorne's solution.

5.4 Area of the Event Horizon

In chapter 4 we briefly mentioned the event horizon of a black hole and it turns out to be of great interest to analyze how the area of the event horizon changes as a function of $\tilde{a}$ and M/M_1 of Kerr black holes.

We shall not dig into the theory here but simply refer to a calculation‡, which shows that the area is given by the equation:

$$A(\tilde{a}, M) = 8\pi \left(\frac{M}{M_1}\right)^2 \left[1 + \left(1 - \tilde{a}^2\right)^{1/2}\right]. \tag{5.37}$$

A plot portraying the contours of Eq. (5.37) is shown in Fig. 5.5, using initial values

*This follows from the discussion in Fig. 5.3 but photons do not travel along timelike geodesics, they travel along null geodesics. An analysis then shows that the values for r_{ISCO} varies from that of particles carrying mass but the same principle still holds.

†In the same paper Thorne provides an illuminating picture which demonstrates the difference between the two situations.

‡For a derivation see Hartle [4], p. 313–316.

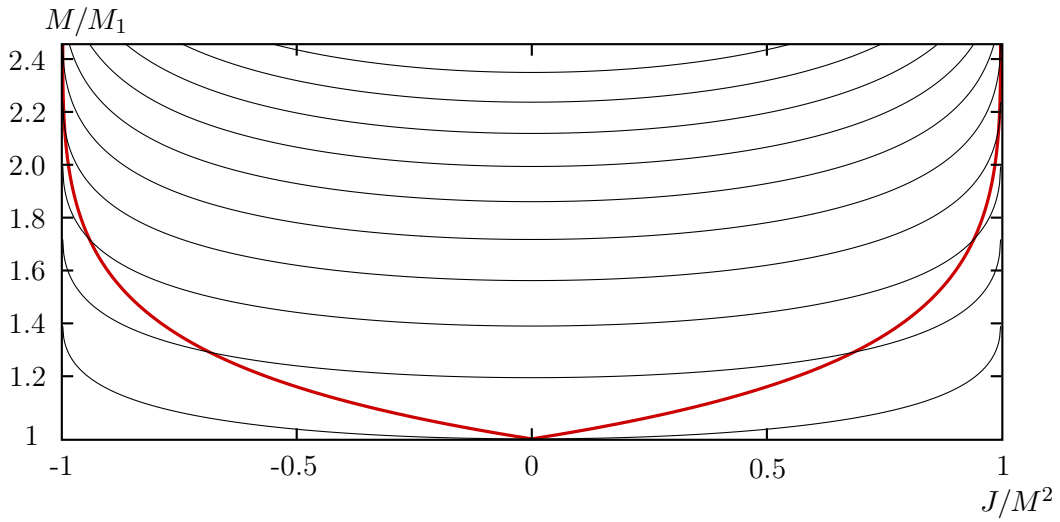

Figure 5.5: A contour plot showing how the area of the event horizon changes as a function of the angular momentum per mass squared $\tilde{a}$ and the mass M/M_1. The red curve from Fig. 5.2 is replotted here along side the contour lines. Each contour represent a certain value of the area of the event horizon, and the intersection of Eq. (5.30) with each contour gives the area for that particular value of $\tilde{a}(M)$. The negative values for the angular momentum are plotted here as well, and they show that precisely the same phenomena occurs for particles in counterrotation.

$M/M_1 = 1$ and $\tilde{a} = 0$ resulting in contours given by $A(\tilde{a}, M) - 16\pi = 0$.

A closer look at the contour lines reveal that in order for the function $A(\tilde{a}, M)$ to remain constant the mass has to increase as the angular momentum per mass squared increases, which is also clear from Eq. (5.37). As we have seen from Fig. 5.2, the mass of black holes increases faster as $\tilde{a} \to 1$, and consequently the area of the event horizon increases faster and faster as the angular momentum per mass squared increases. Thus, the theory seem to imply that the area of the event horizon can only increase with time from the process of disk-accretion we have studied.

It is interesting to note here that the increase in $\tilde{a}$ of black holes actually causes the area of the event horizon to increase. This may seem contradictory, but coupled with an increase in $\tilde{a}$, for the process of disk-accretion we have studied, is also an increase in the mass M which according to Eq. (5.37) has the effect of increasing the area of black holes. Now, Fig. 5.5 tells us that the increase in mass has a greater effect on the increase in area of the event horizon compared to the decrease in area from the increase in angular momentum per mass squared. Recall Fig. 5.2 which is plotted with the contours. If we look for intersections between the contours and $\tilde{a}(M)$ we see that the greater the area is, the higher the angular momentum per mass squared becomes. Consequently we must conclude that the contribution from the increase in mass, is greater than the contribution from an increase in angular momentum per mass squared. In other words; regardless of a decrease in the area of the event horizon from an increase in angular momentum per mass squared, the area of the event horizon still increases.

The reader may object to the usage of Eq. (5.30) in Fig. 5.5 since Bardeen's equation does not seem to give correct values for near extremal black holes. However, Thorne's solution mentioned in section 5.3 deviates from Bardeen's equation only marginally for black holes near the extremal limit. In other words, Fig. 5.5 is accurate to good approximation, and the general principle still holds.

Another interesting remark can be made regarding Thorne's solution. If a black hole starts with an initial value of the angular momentum such that $0.998 \lesssim \tilde{a} \leq 1$, then as we discussed in section 5.3, the black hole begins to spin down and ultimately it settles at the limiting value $\tilde{a} = 0.998$. From Eq. (5.37) it is clear that a decrease in $\tilde{a}$ causes the area

of the event horizon to increase. In this case then, the area of the event horizon ought to be increasing even faster than when the angular momentum per mass squared increases, since the black hole is still accreting matter causing its mass to increase.

It is interesting to make the final remark that according to the laws of black hole thermodynamics derived by Bardeen, Carter and Hawking [20], the area of the event horizon can only increase or remain constant. We must therefore conclude that there is no violation of the second law of black hole thermodynamics from the process of accretion which we have studied.

Chapter 6

Concluding Remarks

In this thesis we have given simple and complete derivations of Eqs. (3.28) provided by Bardeen [12]. It has been shown that a seemingly complicated nonlinear system of equations, which by means of appropriate manipulations, has surprisingly simple solutions which can be found without the use of computer algebraic methods.

In chapter 2 we studied the distribution of the angular momentum of the solar system and found that the total angular momentum per mass squared of the solar system has a value $\tilde{a} \approx 36$. Only a small contribution comes from the rotational angular momentum per mass squared of the Sun, with a value $J/M_{\odot}^2 \approx 0.23$, and the rest from the orbital angular momentum per mass squared of the planets.

If the solar system arose out of a massive gas cloud, there seems to be evidence for the presence of some process which operated on the solar system in its early days, causing most of its angular momentum to be transported to the outer regions.

If indeed stars have an angular momentum per mass squared $\tilde{a} \leq 1$, regardless of their size, then there would be no need for stars to transport their angular momentum to the outer regions of their systems as they approach singularity, since the cosmic censorship hypothesis would not be violated. Instead, the star would compensate its loss in radius by driving up its angular frequency. The star would then have an initial angular momentum per mass squared $\tilde{a} \leq 1$. As time goes on it may happen that the black hole begins to accrete matter which increases its angular momentum per mass squared up to an upper limit. More precisely the upper limit seem to have a theoretical value of $\tilde{a} \approx 0.998$ (in accordance with Thorne, [17]). But it should be mentioned that there is no obvious reason to assume an angular momentum per mass squared $\tilde{a} \leq 1$. There could very well exist massive stars with an angular momentum per mass squared $\tilde{a} > 1$.

In chapter 5 our focus was on the study of matter falling in from the last stable circular orbit at r_{ISCO}, and in the end we briefly mentioned other processes which also have an effect on the angular momentum of black holes. In section 5.2 we mentioned a mechanism which actually decreases the angular momentum. It was there argued that particles falling in from all directions of space has a net effect of decreasing the angular momentum. This happens because counterrotating particles have r_{ISCO} located further away from black holes compared to particles in corotation with black holes, see Fig. 5.1 and Fig. 5.3. This effect grows stronger as the angular momentum per mass squared increases because as $\tilde{a} \to 1$, $r_{\text{ISCO}} \to M$ for corotation and $r_{\text{ISCO}} \to 9M$ for counterrotation. It should also be mentioned that the mechanism we have studied ceases to happen when there no longer is any mass to accrete, it is then possible that the angular momentum per mass squared of black holes decreases as a consequence of matter falling in randomly from all directions of space.

It is interesting to note that the mechanism mentioned above which decreases the angular momentum per mass squared, could very well prevent an accreting supermassive

black hole from increasing its angular momentum per mass squared further when it reaches high values around $\tilde{a} = 0.9$. The process of accretion we have studied is in some sense an isolated form of the real picture, in which we have only looked at one of the contributions to $\tilde{a}$. More precisely, we have assumed that there are no other processes which have an effect on the angular momentum per mass squared. It is not difficult to imagine what could happen if we were to trigger a simulation in which both disk-accretion from r_{ISCO} and random bombardment of matter from all directions of space is taken into account simultaneously. As we have already discussed, Fig. 5.1 tells us that the capture zones for corotating and counterrotating particles differ greatly as the angular momentum per mass squared increases for black holes. In other words, the greater $\tilde{a}$ becomes the more noticeable the effect of a decrease in $\tilde{a}$ from counterrotating particles become. It is then possible that there comes a point when both of these processes has the net effect of canceling each other, ultimately staggering the increase in angular momentum per mass squared causing it to settle at some value $\tilde{a} < 1$.

In section 5.2 we discovered that in order for a black hole to reach an angular momentum per mass squared close to $\tilde{a} = 1$ (recall that the upper limit given by Thorne [17] is $\tilde{a} \approx 0.998$), it needs to accrete matter equivalent to $M/M_1 \sim 6^{1/2}$ of the original mass of the black hole. Consequently an angular momentum close to $\tilde{a} = 1$ may be rare for "ordinary" black holes as they likely do not have enough matter in their surroundings to accrete long enough to reach such high values of $\tilde{a}$. Supermassive black holes on the other hand located at the center of galaxies ought to have a very high angular momentum per mass squared since they exist in very dense regions with large amounts of matter.

Section 5.3 concerned itself with accretion for near extremal black holes. It was there shown that the equation derived by Bardeen [12], Eq. (5.30), behaves in a peculiar manner for near extremal black holes. In fact, the function itself does not seem to give reasonable predictions for values $M/M_1 > 6^{1/2}$, and it is not even defined for values of $M/M_1 > 3$ which at the very least appears strange for black holes which accrete indefinitely. The solution to the problem came from Thorne [17], who apparently was working under a hint from Stephen Hawking that photon emission from the surface of the disk should have an effect on the angular momentum per mass squared. Thorne managed to show that if stress-energy in the form of photon emission from the surface of the disk is also taken into account, the issue essentially goes away in its entirety and even causes black holes to have a limiting value $\tilde{a} < 1$; rendering cosmic censorship inviolable. This happens because the capture zone of photons is greater for photons traveling against the direction of the rotation of the hole than it is for photons traveling in the same direction as the black hole rotates, the net effect of photon capture is thus to reduce the angular momentum per mass squared. Furthermore, Thorne's solution shows that a black hole which begins to accrete with very high values of the angular momentum per mass squared initially $0.998 \lesssim \tilde{a} \leq 1$, spins down very quickly as mass is accreted and settles at the limiting value $\tilde{a} \approx 0.998$.

Following the discussion in the previous paragraph, assume now that a massive star with $\tilde{a} > 1$ is about to collapse and form a black hole, assume furthermore that the angular momentum per mass squared, after the star collapses, still has a value $\tilde{a} > 1$ so that cosmic censorship is violated and the singularity of the black hole is naked. If Thorne's solution holds for a black hole with an initial value $\tilde{a} > 1$, then it would mean that the black hole begins to spin down quickly as a consequence of photon capture, and settle at the limiting value $\tilde{a} \approx 0.998$. In other words, the black hole would have a naked singularity in its early life visible to observers, and ultimately acquire an event horizon as accretion goes on; hiding the singularity from observers. However, it has been shown by Wald [21], that an extremal black hole cannot capture a particle which carries an orbital angular momentum large enough for the resulting spacetime to violate cosmic censorship. Such particles are repelled from the black by centrifugal repulsion. Evidently then for hypothetical stars

with an angular momentum per mass squared $\tilde{a} > 1$ not to violate cosmic censorship upon collapse, there has to exist some process which transports angular momentum to outer regions near the end of their lives.

Consider a massive star which is at the end of its life. As it uses heavier elements as thermonuclear fuel, it swells up into a red giant. Large portions of the stars matter is then located far out from its center and consequently some of its angular momentum has been transported to outer regions. As the star approaches singularity, the angular frequency of the outer regions could be driven up to ultimately form an accretion disk around the black hole. In this manner, the star drives the angular momentum outwards as a consequence of its fusion processes, and then begins to accrete the same matter after the star has become a black hole.

Regardless of whether the process mentioned above is realizable or not; it should be clear that for stars with an angular momentum per mass squared $\tilde{a} > 1$, which ultimately become black holes, there has to exist some process which transports angular momentum to the outer regions in order for them not to violate cosmic censorship. One cannot help to ask whether the same, or some very similar process which operated on the solar system in its early days to transport angular momentum outwards, also operates on black holes as they approach singularities.

Bibliography

[1] Herbert Goldstein, Charles Poole & John Safko, *Classical Mechanics*, Third Edition, Addison Wesley, ISBN: 0–201–65702–3, 2002

[2] Vladimir I. Arnold, *Mathematical Methods of Classical Mechanics*, Second Edition, Springer, ISBN: 978-0-387-96890-2, 1989

[3] Ingemar Bengtsson, *Notes on Analytical Mechanics*, `http://www.fysik.su.se/~ingemar/anmek.pdf`, 2015

[4] James B. Hartle, *Gravity: An Introduction to Einstein's General Relativity*, Addison Wesley, ISBN: 0–8053–8662–9, 2003

[5] Steven Weinberg, *Gravitation and Cosmology: Principles and Applications of the General Theory of Relativity*, John Wiley & Sons, ISBN: 0–471–92567–5, 1972

[6] Ingemar Bengtsson, *Notes on Electrodynamics*, `http://www.fysik.su.se/~ingemar/El02.pdf`, 2002

[7] Monika Mościbrodzka et al, *Radiative Models of Sgr A* from GRMHD Simulations*, arXiv:0909.5431v1, 2009

[8] Jeffrey E. McClintock et al, *Measuring the Spins of Accreting Black Holes*, arXiv:1101.0811v2, 2011

[9] Roy Patrick Kerr, *Gravitational Field of a Spinning Mass as an Example of Algebraically Special Metrics*, Phys. Rev. Letters, **Vol. 11**, p. 237, 1963

[10] Robert H. Boyer & Richard W. Lindquist, *Maximal Analytic Extension of the Kerr metric*, Journal of Mathematical Physics, **Vol. 8**, p. 265, 1967

[11] Donald Lynden-Bell, *Galactic Nuclei as Collapsed Old Quasars*, Nature, **Vol. 223**, p. 690, 1969

[12] James M. Bardeen, *Kerr Metric Black Holes*, Nature, **Vol. 226**, p. 64, 1970

[13] Rachel Howe, *Solar Interior Rotation and its Variation*, arXiv:0902.2406, 2009

[14] J. Christensen-Dalsgaard et al, *The Current State of Solar Modeling*, Science, **Vol. 272**, p. 1286, 1996
Data: `http://astro.phys.au.dk/~jcd/solar_models/cptrho.l5bi.d.15c`

[15] Maria Pia Di Mauro, *Helioseismology: a Fantastic Tool to Probe the Interior of the Sun*, arXiv:1212.5077v1, 2012

[16] James M. Bardeen, William H. Press and Saul A. Teukolsky, *Rotating Black Holes: Locally Nonrotating Frames, Energy Extraction, and Scalar Synchrotron Radiation*, The Astrophysical Journal, **Vol. 178**, p. 347, 1972

[17] Kip S. Thorne, *Disk-accretion Onto a Black Hole*, The Astrophysical Journal, **Vol. 191**, p. 507, 1974

[18] Brandon Carter, *Global Structure of the Kerr Family of Gravitational Fields*, Physical Review, **Vol. 174 5**, p. 1559–1571, 1968

[19] Martin Rees, Remo Ruffini & John Archibald Wheeler, *Black Holes, Gravitational Waves and Cosmology*, Gordon and Breach Science Publishers, ISBN: 0–677–04580–8, 1975

[20] James M. Bardeen, Brandon Carter & Stephen Hawking, *The Four Laws of Black Hole Mechanics*, Communications in Mathematical Physics, **Vol. 32 2**, p. 161, 1973

[21] Robert Wald, *Gedanken Experiments to Destroy a Black Hole*, Annals of Physics, **Vol. 83**, p. 548, 1974